Mon. Not. R. Astron. Soc. **000**, 1–24 (2002) Printed 28 June 2012 (MN LATEX style file v2.2)

Origin of the anti-hierarchical growth of black holes

Michaela Hirschmann[1,2⋆], Rachel S. Somerville[3], Thorsten Naab[4], Andreas Burkert[2]
[1] *INAF - Astronomical Observatory of Trieste, via G.B. Tiepolo 11, I-34143 Trieste, Italy*
[2] *Universitäts Sternwarte München, Scheinerstr.1, D-81679 München, Germany*
[3] *Department of Physics and Astronomy, Rutgers, The State University of New Jersey, 136 Frelinghuysen Rd, Piscataway, NJ*
[4] *Max-Plank-Institute für Astrophysik, Karl-Schwarzschild Strasse 1, D-85740 Garching, Germany*

Accepted ???. Received ??? in original form ???

ABSTRACT

Observational studies have revealed a "downsizing" trend in black hole (BH) growth: the number densities of luminous AGN peak at higher redshifts than those of faint AGN. This would seem to imply that massive black holes formed before low mass black holes, in apparent contradiction to hierarchical clustering scenarios. We investigate whether this observed "downsizing" in BH growth is reproduced in a semi-analytic model for the formation and evolution of galaxies and black holes, set within the hierarchical paradigm for structure formation (Somerville et al. 2008; S08). In this model, black holes evolve from light seeds ($\sim 100 M_{\odot}$) and their growth is merger-driven. The original S08 model (baseline model) reproduces the number density of AGN at intermediate redshifts and luminosities, but underproduces luminous AGN at very high redshift ($z > 3$) and overproduces them at low redshift ($z < 1$). In addition, the baseline model underproduces low-luminosity AGN at low redshift ($z < 1$). In order to solve these problems, we consider several modifications to the physical processes in the model: (1) a 'heavy' black hole seeding scenario (2) a sub-Eddington accretion rate ceiling that depends on the cold gas fraction, and (3) an additional black hole accretion mode due to disk instabilities. With these three modifications, the models can explain the observed downsizing, successfully reproduce the bolometric AGN luminosity function and simultaneously reproduce galaxy and black hole properties in the local Universe. We also perform a comparison with the observed soft and hard X-ray luminosity functions of AGN, including an empirical correction for torus-level obscuration, and reach similar conclusions. Our best-fit model suggests a scenario in which disk instabilities are the main driver for moderately luminous Seyfert galaxies at low redshift, while major mergers are the main trigger for luminous AGN.

Key words: keywords

1 INTRODUCTION

It has been known since early optical quasar surveys that the co-moving number density of luminous quasars has a pronounced peak at a redshift around $z = 2$-2.5 (Schmidt & Green 1983; Boyle et al. 1988; Hewett et al. 1994; Boyle et al. 2000; Warren et al. 1994; Schmidt et al. 1995), with a fairly steep decline at higher and lower redshift. More recently, it was discovered that very massive BH ($10^9 M_{\odot}$) appear to exist already at $z \sim 6$ and higher (Fan et al. 2000, 2001; Mortlock et al. 2011), but they are extremely rare, in accordance with this trend. Recent progress in detecting faint and obscured AGN has been achieved by analysing data from X-ray surveys (XMM-Newton, Chandra, ROSAT, ASCA, e.g. Miyaji et al. 2000; La Franca et al. 2002; Cowie et al. 2003; Fiore et al. 2003; Barger et al. 2003; Ueda et al. 2003; Hasinger et al. 2005; Barger & Cowie 2005; Sazonov & Revnivtsev 2004; Nandra et al. 2005; Ebrero et al. 2009; Aird et al. 2010; Fiore et al. 2012). All of these studies in the hard and soft X-ray range find that the cosmic evolution of AGN is strongly dependent on the AGN luminosity: the number density of successively less luminous AGN peaks at lower redshifts, with the lowest luminosity AGN showing a basically constant number density. Making the simplified assumption that AGN luminosity is proportional to BH mass (as we would expect if black holes are accreting at the Eddington rate, $L \propto M_{\bullet}$) would imply that very massive black holes seem to be already in place at very early times, whereas less massive black holes seem to evolve predominantly at

⋆ E-mail: mhirsch@oats.inaf.it

lower redshifts. This behavior is called 'downsizing' or 'anti-hierarchical' growth of black holes. The downsizing trend is also seen in the optical (Cristiani et al. 2004; Croom et al. 2004; Fan et al. 2004; Hunt et al. 2004; Richards et al. 2006; Wolf et al. 2003) and the NIR (e.g. Matute et al. 2006).

On the face of it, this observational result seems to be in conflict with the expectations within the currently favored hierarchical structure formation paradigm, such as those based on the Cold Dark Matter (CDM) model (Peebles 1965; White & Rees 1978; Blumenthal et al. 1985). In this framework, low mass halos form first and more massive halos grow over time via subsequent merging and smooth accretion. However it is now well known that the evolutionary history of observable *galaxies* also follows an "anti-hierarchical" or downsizing behavior, with several independent observational indicators suggesting that more massive galaxies formed their stars and had their star formation "quenched" earlier than low-mass galaxies, which continue forming stars to the present day (an overview of these observations is given in Fontanot et al. 2009).

Present-day spheroidal galaxies host supermassive black holes at their centers (Magorrian et al. 1998; Genzel & Eckart 1999) and strong correlations have been found between black hole masses and properties of their host galaxies (Ferrarese & Merritt 2000; Gebhardt et al. 2000; Tremaine et al. 2002; Häring & Rix 2004). This can be interpreted as evidence for co-evolution between the host galaxies and their black holes, but some observations of BH growth and SF in individual objects appear to contradict the picture of simple one-to-one co-evolution over time (Mullaney et al. 2012). Thus the details of BH and galaxy co-evolution remain unclear.

During their lifetime, black holes are assumed to undergo several episodes of significant gas accretion, during which this accretion powers luminous quasars or active galactic nuclei (AGN) (Salpeter 1964; Zel'Dovich 1964; Lynden-Bell 1969). By estimating the total energy radiated by AGN over their whole lifetime, it can be shown that nearly all the mass seen in dormant black holes today can be accumulated during the periods of observed bright AGN activity (Soltan 1982). This implies that there is not a great deal of room for "dark" or obscured accretion.

A large number of works have explored the predictions of the ΛCDM model for the formation and evolution of supermassive black holes and AGN, with varying levels of complexity. Several works made predictions based on nearly purely analytic models (Efstathiou & Rees 1988; Haehnelt & Rees 1993; Haiman & Loeb 1998) and on semi-empirical models (Shankar et al. 2009, 2010, 2012) and a large number of studies have been published based on semi-analytic models of galaxy formation within which mechanisms for black hole formation and evolution have been included (e.g. Kauffmann & Haehnelt 2000; Volonteri et al. 2003; Granato et al. 2004; Menci et al. 2004; Bromley et al. 2004; Croton 2006; Bower et al. 2006; Marulli et al. 2008; Somerville et al. 2008). Recently, numerical hydrodynamic simulations have also included black hole growth and AGN feedback using "sub-grid" recipes (Springel et al. 2005; Hopkins et al. 2006; Di Matteo et al. 2005; Robertson et al. 2006; Li et al. 2007; Sijacki et al. 2007; Johansson et al. 2009; McCarthy et al. 2010, 2011; Degraf et al. 2011; Di Matteo et al. 2012). Hopkins et al. (2008) presented predictions based on "semi-empirical" models in which galaxy properties were taken from observations and the relationship between galaxy properties and AGN luminosity was based on the results of a large suite of hydrodynamic merger simulations.

These models differ in many of the details of how BH formation and growth are implemented, but there seems to be a broad consensus on several points. First, self-regulated black hole growth, perhaps via radiation pressure driven winds (Di Matteo et al. 2005; King 2005; Murray et al. 2005; Robertson et al. 2006) is a widely adopted means of obtaining the observed tight relationship between BH mass and spheroid mass (although some models simply assume this relationship without invoking a physical mechanism). Second, one must invoke a physical mechanism that can feed large amounts of gas onto the central BH within a short time. Galaxy-galaxy mergers are a popular (though not universally adopted) way to remove angular momentum from the gas and efficiently drive it to the center of the galaxy. Third, some mechanism must be adopted that reduces or stops gas cooling and accretion in massive dark matter halos. Many models assume that low levels of accretion onto SMBH can produce radio jets that heat the surrounding hot halo (Croton 2006; Bower et al. 2006; Somerville et al. 2008) thereby inhibiting cooling flows, preventing over-massive galaxies from forming and quenching star formation in massive galaxies, leading to more observationally consistent color-magnitude or SFR-stellar mass relationships (Kimm et al. 2009).

However, several aspects of the physics of black hole growth and formation remain poorly understood. First, there are active ongoing debates about when and how seed black holes form: either via a direct collapse of cold gas clouds leading to massive seeds of $\sim$ 10^4-$10^5 M_\odot$ (Loeb & Rasio 1994; Koushiappas et al. 2004; Volonteri & Stark 2011; Bellovary et al. 2011) or via stellar remnants from Pop III stars, resulting in low mass ($\sim$ $100 M_\odot$) black hole seeds (Madau & Rees 2001; Heger & Woosley 2002). An alternative possibility is direct seed formation in a merger event as seen in the numerical simulations of Mayer et al. (2010). While the seeding mechanisms do not alter the AGN and black hole population at low redshift (as gas accretion during the evolution exceeds the seed black hole masses by many orders of magnitude), at high redshift the choice of the seeding model strongly influences the black hole formation and is highly relevant for understanding the observed population of luminous high redshift quasars.

Another matter of vigorous debate is the process or processes that trigger and regulate accretion onto the central SMBH. As noted above, the most luminous observed quasars require accretion rates such that $\sim 10^8$–$10^9 M_\odot$ of gas must be funneled onto the black hole over a timescale of $< 10^{8.5}$ yr, i.e. nearly the whole gas content of a good-sized galaxy must be fed onto the black hole in roughly a dynamical time (see discussion in Hopkins et al. 2008, and references therein). Mergers appear to be a physically well-motivated candidate for producing this dramatic effect, and semi-empirical calculations have shown that there is a statistical consistency between the observed merger rate and the observed AGN duty cycle and luminosity function (Hopkins et al. 2006, 2008), suggesting that it is at least

possible that these processes are causally linked. However, the observational situation remains murky. Observational studies have repeatedly failed to find evidence for a statistically significant enhancement of merger-related signatures, such as close pairs or morphological disturbance, in AGN hosts up to $z \sim 1$ (Cisternas et al. 2010; Georgakakis et al. 2009; Pierce et al. 2007; Grogin et al. 2005; Li et al. 2008; Ellison et al. 2008). But a recent study by Ellison et al. (2011) does find a significant enhancement of AGN activity in close pairs, and discusses reasons that previous studies based on similar data have not found a signal. The absence of enhanced merger signatures in morphological studies has recently been shown to persist in X-ray selected AGN up to $z \sim 2.5$ (Schawinski et al. 2011; Kocevski et al. 2012). Recent work suggests, though, that the fraction of hosts with morphological disturbances may be higher in obscured AGN, many of which are missing from X-ray selected surveys (S. Juneau, private communication).

The goal of this work is to explore the the interplay of different physical processes that determine the masses of seed black holes, the triggering of AGN activity and the efficiency of gas accretion during the active phases of black holes, with the aim of understanding the physical origin of the observed downsizing trend in black hole growth. We follow a semi-analytic approach, which has been shown to successfully reproduce many observed galaxy population properties (Somerville et al. 2008, Somerville et al. 2011) and includes a model for the merger triggered formation and evolution of black holes (see Section 3 for details). In this paper we present three major modifications to the baseline model published in S08:

- gas fraction dependent Eddington ratios (accretion efficiency)
- AGN activity triggered by disk instabilities
- 'heavy' black hole seeds

to the existing model. We find that with these three modifications, our model does reproduce the observed downsizing behavior.

In Section 2 we briefly summarize the results from previous studies. Section 3 gives a brief overview of the semi-analytic model used in our study and describes the different modifications for black hole growth we are considering. In Sections 4 and 5 we present some properties of present-day and high-redshift galaxies and their black holes, which are compared to observations. The AGN number density evolution is studied in Section 6, considering the influence of the different modifications concerning black hole growth. Section 7 presents a comparison of the evolution of the observed bolometric and hard and soft X-ray luminosity function with the model output. In Sections 8 and 9, we discuss the evolution of the Eddington ratio distributions and the evolution of the black hole-AGN luminosity plane. Finally, in Section 10, we summarize and discuss our main results.

2 PREVIOUS STUDIES

A number of studies have investigated the observed anti-hierarchical trend of BH activity using the 'Galform' (Durham) (Bower et al. 2006), the 'Munich' (De Lucia & Blaizot 2007) or the 'Morgana' semi-analytic models (Monaco & Fontanot 2005; Fontanot et al. 2006). The first two models are applied to the dark matter merger trees of the Millennium simulation, while the latter uses merger trees from the Pinocchio method. All models distinguish between black hole accretion in the bright quasar mode and the low-Eddington ratio radio-mode. In the 'Galform' model, the quasar mode is triggered by merger events *and* disk instabilities, but the mass growth of black holes is dominated by accretion due to disk instabilities. In the 'Munich' model the quasar mode is assumed to be triggered *only* by merger events. The 'Morgana' model assumes that any low angular momentum gas within the "bulge" gas reservoir is available to accrete onto the central BH. Gas may be transferred to the "low-J" reservoir either by mergers or disk instabilities. In this model, black holes grow at a rate determined by the viscosity of the accretion disk and the mass of gas in the low-J reservoir. In the 'Galform'-model the black hole accretion rate is proportional to the star formation rate during a starburst (triggered either by a merger or disk instability), whereas in the 'Munich'-model the accretion rate is dependent on the cold gas content in the galaxy, the galaxy circular velocity, and the mass ratio of the triggering merger. **While these recipes differ in detail, they are both proportional to the gas content and rougly inversely proportional to $(1+V_c^{-2})$, where V_c is the circular velocity of the bulge component in the case of 'Galform' and the halo virial velocity in the 'Munich'-model, and both lead to a black hole-bulge mass relation at $z = 0$ that is consistent with the observed one. However, it appears that the history of black hole accretion is significantly different in the two models.** In the 'Morgana'-model, black holes grow at a rate determined by the viscosity of the accretion disk and the mass of gas in the low-J reservoir.

Fontanot et al. (2006) claim that their 'Morgana'-model can reproduce downsizing, which in their model is caused by stellar kinetic feedback that arises in star-forming bulges leading to a removal of cold gas in small elliptical galaxies (reduction of the number of faint AGN at high redshift). To obtain a good match to the number density of bright quasars they require quasar-triggered galactic winds, which self-limit the accretion onto black holes.

Malbon et al. (2007) found, using the 'Galform' semi-analytic code, that the direct accretion of cold gas during starbursts is an important growth mechanism for lower mass black holes and and for all black holes at high redshift. The assembly of pre-existing black hole mass into larger units via merging dominates the growth of more massive black holes at low redshift. Therefore, they claim that as redshift decreases, progressively less massive black holes have the highest growth rates, in agreement with downsizing. Their model output reproduces the evolution of the optical luminosity function of quasars, however, they do not show a quantitative comparison for the X-ray and/or bolometric AGN luminosity.

Fanidakis et al. (2010) have constructed a model based on the 'Galform'-model framework, but with different recipes for black hole growth and AGN feedback. They present a quantitative comparison of their model output to the observed quasar luminosity function at different redshifts. **The previous 'Galform'-based SAMs associated radiatively efficient BH accretion with "cold**

mode" accretion (merger or disc-instability triggered) and radiatively inefficient accretion with "hot mode" accretion (accretion from a quasi-hydrostatic hot gas halo). In contrast, Fanidakis et al. (2010) associate accretion at low accretion rates (less than about one percent of the Eddington rate), regardless of its origin, with radiatively inefficient advection dominated accretion flows (ADAF), and assume that accretion at higher rates will be radiatively efficient. At high redshift, Fanidakis et al. (2010) do not Eddington-limit the accretion rates, but allow super-Eddington accretion, which is responsible for very luminous AGN at high redshifts. The high number density of low luminosity AGN at low redshift can be explained by the luminosity produced via the ADAF mode. They attribute the observed downsizing trend mainly to dust obscuration of low luminosity AGN at high redshift.

Marulli et al. (2008) investigated different parameterizations of the quasar light curves in the 'MUNICH'-model, and found as expected, that the lightcurve parameterization has a large effect on the number density of faint AGN as a function of redshift. They found the best results with a lightcurve model that includes an Eddington growth phase followed by a power-law decline phase as suggested by Hopkins et al. (2006). However, for all adopted lightcurve models they found that the previously published Munich model underpredicts the number density of luminous quasars at high redshift ($z > 1$). Finally, in a follow-up study by Bonoli et al. (2009), the BH accretion efficiency was assumed to be a function of redshift as well as gas content and merger mass ratio. They obtained improved results, but still were not able to reproduce the luminosity function of observed AGN over the full range in redshift and luminosity.

3 THE SEMI-ANALYTIC MODEL

The semi-analytic model used in this study is presented in S08 and we refer the reader to this paper for details. The galaxy formation model is based on dark matter merger trees generated by the extended Press-Schechter formalism. The evolution of baryons within these dark matter halos is modeled using prescriptions for gas cooling, reionization, star formation, supernova feedback, metal evolution, black hole growth and AGN feedback. Here we focus on the mechanism describing the formation and evolution of black holes. *Each* top-level dark matter halo is seeded with a 100 $M_\odot$ black hole in its center, which can grow by two mechanisms: through cold gas accretion during the 'bright' quasar mode and through accretion of gas from the hot halo via a cooling flow during the low-Eddington ratio and radiatively inefficient radio mode. The quasar mode is assumed to produce momentum-driven winds, which are modeled using the analytic scaling derived and calibrated from binary hydrodynamic merger simulations (Robertson et al. 2006; Cox et al. 2006a; Robertson et al. 2006; Hopkins et al. 2007b; Robertson et al. 2006).

The radio mode can only occur when a hot quasi-hydrostatic halo is present, which is assumed to be the case when the cooling shock is predicted to be within the virial radius ($r_{\rm cool} < r_{\rm vir}$). During this phase, black holes are fuelled by Bondi-Hoyle-accretion (Bondi 1952), with the isothermal cooling-flow solution from Nulsen & Fabian (2000). The growth in the radio mode is also associated with an efficient production of radio jets that results in an energy injection into the intracluster medium (ICM). Therefore, we assume that the energy arising from the accretion onto the black hole couples to and heats the gas in the surrounding hot halo (Radio mode feedback).

3.1 Standard accretion model

The quasar phase is triggered by galaxy merger events with a mass ratio of $\mu > 0.1$, where μ is the mass ratio of the baryonic components and the dark matter within the central part of the galaxy (see S08 for the precise definition). The lower limit is motivated by binary hydrodynamic merger simulations. Whenever the two progenitor galaxies merge, their black holes are assumed to also merge and form a single black hole whose mass is the sum of the progenitor BH's masses. The model for gas accretion onto the black hole is motivated by the analysis of gas inflow rates onto the nuclear regions from idealized disk merger simulations (Springel et al. 2005; Robertson et al. 2006; Cox et al. 2006b; Hopkins et al. 2006, 2007a). During the merger, the BH is assumed to grow rapidly with accretion rates near the Eddington limit. This rapid accretion continues until the energy being deposited into the ISM in the central region of the galaxy is sufficient to significantly offset and eventually halt accretion via a pressure-driven outflow. During this "blow-out" phase, the accretion rate declines gradually until the nuclear fuel is exhausted.

Based on the merger simulations, the final black hole mass $M_{\bullet,\rm final}$ at the end of the blow-out phase is assumed to be related to the mass of the spheroidal component after the merger:

$$M_{\bullet,\rm final} = f_{\rm BH,final} \times 0.158 \left(\frac{M_{\rm sph}}{100 M_\odot}\right)^{1.12} \times \Gamma(z). \quad (1)$$

Here, $M_{\rm sph}$ is the final spheroid mass after the merger, $f_{\rm BH,final}$ is an adjustable parameter and $\Gamma(z)$ describes the evolution of the black hole-bulge mass relation with time (Hopkins et al. 2006). Following the merger simulations, a Gaussian distributed scatter with a value of $\sigma_\bullet = 0.3$ dex is additionally applied to the accreted gas mass, representing stochasticity due to e.g. the properties of the orbit. When the black hole mass has reached its final mass value, the quasar mode is switched off. During the quasar phase, the light curve models describe two different growth regimes: an Eddington-limited and a power-law decline phase of accretion. In the first regime, the black hole accretes at the Eddington limit until it reaches a critical black hole mass $M_{\bullet,\rm crit}$:

$$M_{\bullet,\rm crit} = f_{\rm BH,crit} \times 1.07 \left(M_{\bullet,\rm final}\right)^{1.1}. \quad (2)$$

Here, the parameter $f_{\rm BH,crit}$ is set according to the merger simulations, and determines how much of the black hole growth occurs in the Eddington-limited versus power-law decline phase. The growth of the black hole during the first regime can be modeled by an exponential increase of mass:

$$M_{\bullet,\rm new}(t) = M_\bullet \exp\left(\frac{1-\epsilon}{\epsilon} f_{\rm edd} \frac{t}{t_{\rm salp}}\right), \quad (3)$$

where $\epsilon = 0.1$ is the efficiency of the conversion of rest mass to energy, and $t_{\rm salp} \approx 0.45$ Gyr is the Salpeter timescale. No strong observational constraints are available for ϵ and if or how it evolves with redshift. However, some observations at $z = 0$ indicate that $0.04 < \epsilon < 0.16$ (Marconi et al. 2004). For simplicity we take a constant mean value of $\epsilon = 0.1$ at all redshifts, which is a very standard assumption. The parameter $f_{\rm Edd}$ in Eq. 3 is the maximum accretion rate, which is defined by the ratio of bolometric luminosity to the Eddington luminosity:

$$f_{\rm Edd} = L_{\rm bol}/L_{\rm Edd}. \quad (4)$$

The Eddington luminosity $L_{\rm Edd}$ (assuming a hydrostatic equilibrium between the inward gravitational force and the outward radiation pressure) is given by:

$$L_{\rm Edd} = \frac{4\pi G M_\bullet m_p\, c}{\sigma_T} = 1.4 \times 10^{46} \left(\frac{M_\bullet}{10^8 M_\odot}\right) {\rm erg/s}, \quad (5)$$

where σ_T is the Thomson cross section for an electron and m_p the mass of a proton. Combining eq. 3, 4 and 5 and the relation $L_{\rm bol} = \epsilon/(1-\epsilon)\dot{M}c^2$, the corresponding accretion rate in the first regime can be calculated by:

$$\dot{M}_{\bullet,I}(t) = 1.26 \times 10^{38} {\rm erg/s}\ \frac{1-\epsilon}{\epsilon} \frac{f_{\rm edd}}{c^2} M_{\bullet,{\rm new}}(t). \quad (6)$$

Note that in the baseline model, the maximum accretion rate is assumed to equal the Eddington rate, i.e. $f_{\rm Edd} = 1$.

Once it exceeds the critical mass $M_{\bullet,{\rm crit}}$ in Eq. 2, the black hole enters the second regime, the 'blow-out' phase, which is described by a power-law decline in the accretion rate. Fitting the light curves in merger simulations from Hopkins et al. (2006) gives the following parametrization for $\dot{M}_{\bullet,II}$:

$$\dot{M}_{\bullet,II}(t) = \frac{\dot{M}_{\bullet,{\rm peak}}}{1 + (t/t_Q)^\beta} \quad (7)$$

where $t_Q \propto t_{\rm salp}$ is the e-folding time, $\dot{M}_{\bullet,{\rm peak}}$ is the peak accretion rate (given by $f_{\rm Edd}$ times the Eddington accretion rate) and β is a parameterized function of the peak accretion rate. In the case that the initial black hole mass is already larger than the calculated critical mass, the black hole is not allowed to accrete at the Eddington rate at all and goes immediately into the blow-out phase. If the initial black hole is even larger than the calculated final mass, no quasar phase occurs at all. Note that for calculating the bolometric luminosity only the accretion rates during the quasar phases are taken into account (thus ignoring the contribution from the radio mode accretion):

$$L_{\rm bol} = \frac{\epsilon}{1-\epsilon}\ \dot{M}_{\bullet,{\rm QSO}}\ c^2 \quad (8)$$

where $\dot{M}_{\bullet,{\rm QSO}} = \dot{M}_{\bullet,I}$ in regime I and $\dot{M}_{\bullet,{\rm QSO}} = \dot{M}_{\bullet,I}$ in regime II.

3.2 Sub-Eddington limit for the maximum accretion rate

Observational studies show that the peak in the Eddington ratio distributions of QSOs is not constant with time; instead, it is found to be dependent on redshift as well as on black hole mass (Padovani 1989; Vestergaard 2003; Shankar et al. 2004; Kollmeier et al. 2006; Netzer & Trakhtenbrot 2007; Hickox et al. 2009; Schulze & Wisotzki 2010). In particular at low redshifts $z < 1$, it has been claimed that there is a *sub-Eddington* limit for black hole accretion, which is dependent on black hole mass and redshift (e.g. Netzer & Trakhtenbrot 2007; Steinhardt & Elvis 2010). The underlying reason for such a sub-Eddington limit is not obvious but might be related to the cold gas content of the galaxy. For example, Hopkins et al. (2008) found, in their semi-empirical models, that allowing 'dry' (gas-poor) mergers to trigger quasar activity would overproduce luminous quasars at low redshift ($z < 1$). To explore this effect we introduce a limit for the Eddington ratio at $z \leqslant 1$, which is dependent on the cold gas fraction $f_{\rm cold} = M_{\rm cold}/(M_{\rm cold} + M_{\rm stellar})$ of the merged galaxy after the merger. For $f_{\rm cold} > 0.3$, we still allow the black hole to accrete up to the Eddington-rate, while for $f_{\rm cold} < 0.3$ we assume a simple, linearly decreasing function for the maximum accretion rate:

$$f_{\rm Edd}(f_{\rm cold}) = 3.3 \times f_{\rm cold} + 0.001 \quad (9)$$

This lowers the peak accretion rate, and therefore also correspondingly decreases the accretion rate in the power-law decline part of the light curve. Note that the assumption of a limited accretion rate is also supported by the results of semi-empirical models by Shankar et al. (2011), which also favor a decreasing Eddington-ratio with time and a radiative efficiency increasing with black hole mass.

3.3 Disk instabilities

Various observational studies suggest that moderately luminous AGN are typically not major-merger driven, at $z < 1$ (Cisternas et al. 2010; Georgakakis et al. 2009; Pierce et al. 2007; Grogin et al. 2005), and interestingly also at $z \approx 2$ (Kocevski et al. 2012; Rosario et al. 2011; Silverman et al. 2011) as they do *not* find more morphological distortions for AGN host galaxies than for inactive galaxies. This suggests that moderately luminous AGN may undergo a 'main sequence' secular growth, e.g. their nuclear activity might be additionally driven by disk instabilities. Here we use a statistic proposed by Efstathiou et al. (1982) to quantify disk stability, based on numerical N-body simulations. They find that the disk becomes unstable if the ratio of dark matter mass to disk mass becomes smaller than a critical value, and give the following parameterization for the onset of disk instabilities:

$$M_{\rm disk,crit} = \frac{v_{\rm max}^2\ R_{\rm disk}}{G\ \epsilon}, \quad (10)$$

where $M_{\rm disk,crit}$ is the critical disk mass, above which the disk is assumed to become unstable, $v_{\rm max}$ is the maximum circular velocity, $R_{\rm disk}$ the exponential disk length and ϵ the stability parameter. We use a slightly smaller value ($\epsilon = 0.75$) than proposed in Efstathiou et al. (1982), **as it results in a better quantitative match with the observed AGN luminosity function (see section 6). However, we find that the number density of AGN is not very sensitive to the precise value of the stability parameter. A smaller stability parameter means that the critical disk mass becomes slightly larger and thus, on average disks become unstable at a later time, leading to a minor decrease in the num-**

ber density of instability-driven AGN. Moreover, we have seen that recent simulations of isolated disk galaxies tend to indicate an even smaller stability parameter of $\epsilon \sim 0.6$. Furthermore, in our model it is assumed that whenever the current disk mass (consisting of both stars and cold gas) exceeds the critical disk mass, the bulge component is enlarged by the difference of the 'excess' stellar mass $\Delta M_{\rm disk} = M_{\rm disk} - M_{\rm disk,crit}$ so that the disk becomes stable again. We assume that a certain amount of cold gas (proportional to the excess disk mass) is additionally accreted onto the black hole triggering an active phase:

$$M_{\rm diskfuel} = f_{\rm BH,disk} \times \Delta M_{\rm disk}. \quad (11)$$

Here, we adopt $f_{\rm BH,disk} = 10^{-3}$, motivated by the local black hole-bulge mass relation. For the accretion process we assume a constant Eddington ratio of $f_{\rm edd} = 0.01$ with a Gaussian distributed scatter of 0.02 dex (motivated by observations, D. Alexander private communication). The black hole accretes as long as there is gas fuel from disk instabilities left ($M_{\rm diskfuel} > 0$) and the accretion rate is calculated by:

$$\dot{M}_{\bullet,\rm disk} = 1.26 \times 10^{38} {\rm erg/s} \ \frac{1-\epsilon}{\epsilon} \frac{f_{\rm edd}}{c^2} M_\bullet \quad (12)$$

For the total bolometric luminosity, the bolometric luminosities from the merger driven quasar phase (equation 8) and from any disk instablities are summed up:

$$L_{\rm bol} = \frac{\epsilon}{1-\epsilon} \left(\dot{M}_{\bullet,\rm QSO} + \dot{M}_{\bullet,\rm disk} \right) c^2. \quad (13)$$

In contrast, the studies using the MUNICH model (Marulli et al. 2008; Bonoli et al. 2009) do not consider disk instabilities for calculating the AGN bolometric luminosity. In the GALFORM model, a similar approach is used to estimate when a disk should become unstable, but it is then assumed that *all* gas and stars in the disk are transferred to the bulge component, leading to a much more dramatic effect. As a result, in their model, disk instabilities are found to be the *major* physical process responsible for black hole growth at all redshifts (Bower et al. 2006; Fanidakis et al. 2010).

Our simple model is based on simulations of isolated disk galaxies, which develop secular internal instabilities. These secular instabilities are not expected to be associated with large nuclear inflows nor with dramatic morphological or dynamical transformation. However, in a cosmological context, the expected rapid inflows can lead to more violent "stream fed" disk instabilities, particularly at high redshift, which may drive BH feeding at high rates, and more dramatic morphological/dynamical transformation (Bournaud et al. 2011; Ceverino et al. 2010). However, it is not known how common such violent instabilities might be in a cosmological context, nor how to model their effects within a semi-analytic model. This is an important topic for future work, but for the moment we restrict ourselves to the more mild secular instabilities. The reader should keep in mind, however, that this may represent a minimal prediction for the impact of internal instabilities on AGN feeding and spheroid formation.

3.4 'Heavy' seeding scenario

The origin of the first massive black holes is still a subject of intense debate. Currently, there exist two favored seeding mechanisms (Haiman 2010; Volonteri 2010): either black hole seeds could form out of the remnants of massive Pop III stars (e.g. Madau & Rees 2001; Heger & Woosley 2002) or during the direct core-collapse of a low-angular momentum gas cloud (e.g. Loeb & Rasio 1994; Koushiappas et al. 2004; Volonteri et al. 2008; Volonteri & Stark 2011; Bellovary et al. 2011). In the first case the seeds are expected to have masses of $M_{\rm seed} \approx 100 - 600 M_\odot$ ('light' seeding), while in the latter case, more massive seeds between $M_{\rm seed} \approx 10^5 - 10^6 M_\odot$ ('heavy' seeding) would be expected. The detailed physical processes, in particular of the direct core-collapse, are largely unknown. Unfortunately, observational constraints in the high-redshift universe are too weak to favor one of these models. However, future observations of gravitational waves (LISA, Sesana et al. 2005; Koushiappas & Zentner 2006) or planned X-ray missions (WFXT: Sivakoff et al. 2010; Gilli et al. 2010; IXO), may have the ability to detect accreting black holes at $z > 6$, and thus, will be able to test these models of the first black holes. Moreover, due to the exponential growth of the black holes during accretion, it is also very difficult to use the local population of massive black holes to recover information about their original masses before the onset of accretion. For instance, in the theoretical studies of Volonteri et al. (2008), and Volonteri (2010), the different seeding mechanisms are investigated by following the mass assembly using Monte-Carlo merger trees to the present time. They find that both models can fit observational constraints at $z = 0$ (e.g. the black hole mass-velocity dispersion relation or the black hole mass function), when light seeds form already at very early times ($z = 20$), or when heavy seeds evolve later on ($z = 5 - 10$). Furthermore in a study of Tanaka & Haiman (2009) they use dark matter halo merger trees, coupled with a prescription for the halo occupation fraction and they show that $\approx 100 M_\odot$ seed BHs can grow into $10^6 M_\odot$ BHs at $z \approx 6$ without super-Eddington accretion, but only if they form in minihalos at $z \geqslant 30$. In our baseline model, seed black hole masses of $100 M_\odot$ were assumed, however, due to our adopted mass resolution, we obtain very little seeding before $z \approx 10$. Therefore, we also explore a heavy seeding scenario with $M_{\bullet,\rm seed} = 10^5 M_\odot$. The different seeding mechanisms will not affect the $z = 0$ black hole mass and AGN population, as initial seed masses are compensated by gas accretion growth processes by orders of magnitude. Only the black hole distribution and QSO luminosity function at high redshifts will be influenced by this modification. Furthermore, some studies have suggested that low mass dark matter halos may not be able to produce massive seeds (Menci et al. 2008; Volonteri et al. 2011), as the potential well might be too weak for collapse to occur. Therefore in the 'heavy seeding' model we additionally adopt a halo mass limit of $2 \times 10^{11} M_\odot$, below which no black hole seeds are inserted.

Furthermore, many observations (e.g. Walter et al. 2004; Peng et al. 2006; McLure et al. 2006; Schramm et al. 2008) suggest that the black hole-to-bulge mass ratio was larger at higher redshifts than expected from the local black

hole-bulge mass relation. This eventually implies that black holes were accreting more gas and thus, growing faster than the corresponding bulges at high redshifts than at lower ones. Therefore, besides assuming an evolving black hole-bulge mass relation (see the z-dependent Γ parameter in eq. 1) we additionally adopt a larger scatter $\sigma_{\bullet,\mathrm{accr}}$ for the accreted mass onto the black holes at high redshifts. This means that, when calculating the final black hole mass $M_{\bullet,\mathrm{final}}$, a larger Gaussian distributed scatter is applied with a value of $\sigma_{\bullet,\mathrm{accr}} = 0.6$ for $z > 4$. At redshift $z < 4$ the original scatter value $\sigma_{\bullet,\mathrm{accr}} = 0.3$ is applied. We find that we still recover a tight relationship between BH mass and bulge mass at $z = 0$, in agreement with observations. This is in agreement with the results of Hirschmann et al. (2010), who showed that a large scatter in black hole mass at fixed bulge mass ($\sigma = 0.6$ dex) at high redshift ($z = 3$) will decrease towards the observed present-day value due to mergers.

3.5 Summary of Model Variants

In the course of this study, we investigate the effects of the outlined modifications on the AGN/black hole evolution one-by-one and in various combinations. We consider the following six different models:

1. **FID**: **Fid**ucial, standard accretion model (3.1)
2. **VE**: **V**arying sub-**E**ddington limit for the maximum accretion rate f_{edd} (3.1 & 3.2)
3. **DI**: Additional accretion due to **D**isk **I**nstabilities (3.1 & 3.3)
4. **SH**: Heavy **S**eeding mechanism with a **H**alo mass limit (3.1 & 3.4)
5. **DISH**: **D**isk **I**nstabilities & Heavy **S**eeding mechanism with a **H**alo mass limit (3.1,3.3 & 3.4)
6. **VEDISH**: Best-fit model including a **V**arying sub-**E**ddington limit, **D**isk **I**nstabilities & a heavy **S**eeding mechanism with a **H**alo mass limit (3.1, 3.2, 3.3 & 3.4)

4 PROPERTIES OF NEARBY GALAXIES AND BLACK HOLES

In Fig. 1 we compare different galaxy and black hole properties from the FID, the DISH and the VEDISH model to observations of the local Universe. We do not explicitly show the predictions of the VE, the DI and the SH model separately as they do not result in a stronger deviation from the FID model than the DISH or the VEDISH model.

The upper left panel in Fig. 1 shows the modeled stellar mass functions compared to observations from Bell et al. (2003) and Panter et al. (2007). The modifications in the DISH and the VEDISH model hardly show any variation from the FID model and thus, for stellar masses larger than $10^9 M_\odot$ we obtain a reasonably good match to the observational data. However, low-mass galaxies ($< 10^9 M_\odot$) are slightly over-predicted, a common feature of most (all) current semi-analytic models (e.g. Bower et al. 2006; De Lucia & Blaizot 2007) and still a subject of on-going research (e.g. Guo et al. 2011; Bower et al. 2011; Wang et al. 2011; Menci et al. 2012). Stronger supernova feedback, a modified star formation law or a different cosmological model are currently considered as possible solutions for this problem.

The present-day black hole mass function is depicted in the upper right panel of Fig. 1. Our model predictions are compared with observational estimates from Shankar et al. (2004), Marconi et al. (2004) and Shankar et al. (2009) (see the review of Shankar 2009 for more details). We find reasonably good agreement of the SAM predictions with the observations for the whole black hole mass range. Deviations between the different SAM models are negligible, indicating that neither the growth of black holes by disk instabilities nor the limited accretion rates at low redshifts influence the black hole mass function significantly. In contrast to our result, in many SAM studies an excess of very massive black holes can be seen (e.g. Fontanot et al. 2006; Malbon et al. 2007; Marulli et al. 2008; Fanidakis et al. 2010), which might be caused by too-efficient Radio-mode accretion as discussed by Fontanot et al. (2011).

The present-day relation between black hole and bulge mass is shown in the lower left panel of Fig. 1, with our model predictions compared with the observational relation derived by Häring & Rix (2004). All of the model variants reproduce a tight relationship between black hole mass and bulge mass, which results from the self-regulated BH growth assumed in our model. The slight upturn at low bulge masses in the DISH and the VEDISH models is due to the heavy seeding mechanism, where by construction no black hole masses below $10^5 M_\odot$ can exist.

Finally, the lower right panel of Fig. 1 shows the active black hole mass function predicted by our model, compared with observational data from Greene et al. (2010) and Schulze & Wisotzki (2010). Note that — consistent with these observational studies — we define "active" BH here as having a bolometric luminosity greater than $10^{43.5}$ erg/s. For $M_\bullet < 10^{8.3} M_\odot$, the accretion due to disk instabilities (DISH/VEDISH models) increases the fraction of active black holes by almost one order of magnitude compared to the FID model. In contrast, for $M_\bullet > 10^{8.3} M_\odot$ the limited gas accretion in the VEDISH model reduces the active fraction of massive black holes compared to the DISH and the FID model. Overall, the VEDISH model provides a better match to the observational data than the FID or the DISH models.

5 GALAXY AND BLACK HOLE PROPERTIES AT HIGHER REDSHIFT

Fig. 2 illustrates the stellar mass functions at different redshifts ($z = 0.5, 1, 2, 3, 4, 5$) as indicated in the legend of each panel. We compare our SAM predictions with the results of different observational studies (Pérez-González et al. 2008; Bundy et al. 2005; Drory et al. 2004; Fontana et al. 2006; Marchesini et al. 2007; Ilbert et al. 2010). At all redshifts, there is no significant difference between the different model variants. However, compared to observations, the high mass end is under-predicted, while the low-mass end is over-predicted by the SAMs. This discrepancy is again a well-known problem (Fontanot et al. 2009; Marchesini & van Dokkum 2007). Fontanot et al. (2009) showed this for the Morgana, Munich and the S08 model, and Guo et al. (2011) found the same for the latest ver-

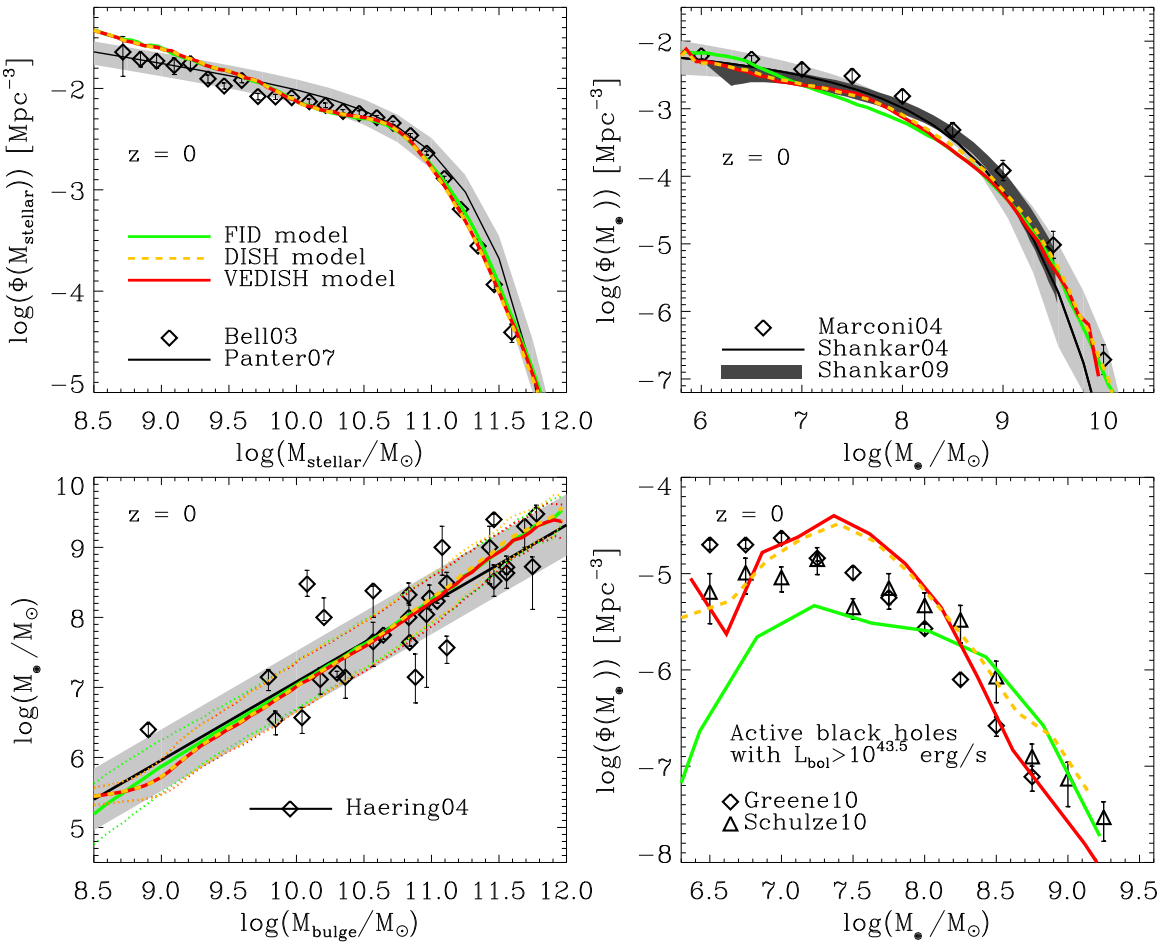

Figure 1. Comparison of SAM results to observations for black hole and galaxy properties of the local Universe. The solid lines are the FID (green) and the VEDISH (red) model, the dashed, orange lines the DISH model. Upper left panel: the stellar mass function. The black solid line and the black symbols show observational results from Panter et al. (2007) and Bell et al. (2003), respectively. Upper right panel: the black hole mass function. Observational estimates (Marconi et al. 2004; Shankar et al. 2004, 2009) are illustrated by the black solid lines, the grey shaded areas and the black symbols. Bottom left panel: black hole-bulge mass relation. The black solid line and symbols correspond to the observed relation by Häring & Rix (2004) and the grey shaded area show the 1-σ scatter of the observational data. Bottom right panel: the mass function of active black holes with bolometric luminosities above $L_{\rm bol} < 10^{43.5}$ erg/s. Open symbols show observations from Greene et al. (2010) and Schulze & Wisotzki (2010). Disk instabilities increase the number of active low mass black holes and the gas-dependent Eddington-limit decreases the number of active high mass black holes.

sion of the Munich model. The discrepancy at the high-mass end may be related to systematic errors or scatter in the photometric stellar mass estimates from observations — Fontanot et al. (2009) showed that when stellar mass errors of 0.25 dex were convolved with the model results, the SAMs agreed reasonably well with the available stellar mass function compilations at least to $z \sim 3$. Moreover, Somerville et al. (2011) showed that the SAM presented here agrees with the observed rest-frame K-band luminosity function at the bright end up to $z \sim 3$. The excess of low mass galaxies at high redshift is also seen in numerical cosmological hydrodynamic simulations (Davé et al. 2011), showing that this problem is not peculiar to SAMs. Instead, it may be an indication that the star formation or supernova feedback recipes that are commonly adopted in both SAMs and numerical simulations require revision (Caviglia & Somerville, in prep.), or that the underlying cosmological model differs from the Cold Dark Matter paradigm (e.g., warm dark matter; Menci et al. 2012).

Fig. 3 shows the black hole mass function at different redshift steps ($z = 0, 0.5, 1, 2, 3, 4, 5, 6$) for the FID, DISH, and VEDISH models. We show the observational estimates at $z = 0$ to guide the eye. At redshifts $z < 3$, the different model assumptions in the DISH and the VEDISH models do not influence the evolution of the black holes. However, turning to higher redshift $z \geqslant 3$, the main difference between the FID model and the DISH/VEDISH models is the larger number density of black holes more massive than $M_\bullet > 10^6 M_\odot$. This can be explained by the 'heavy' seeding scenario and the large scatter in the accreted gas mass onto the black hole at $z > 4$. This leads to larger black hole masses and faster growth at early redshift than in the FID model. Towards lower redshift, however, this effect dissappears as the subsequent growth by gas accretion

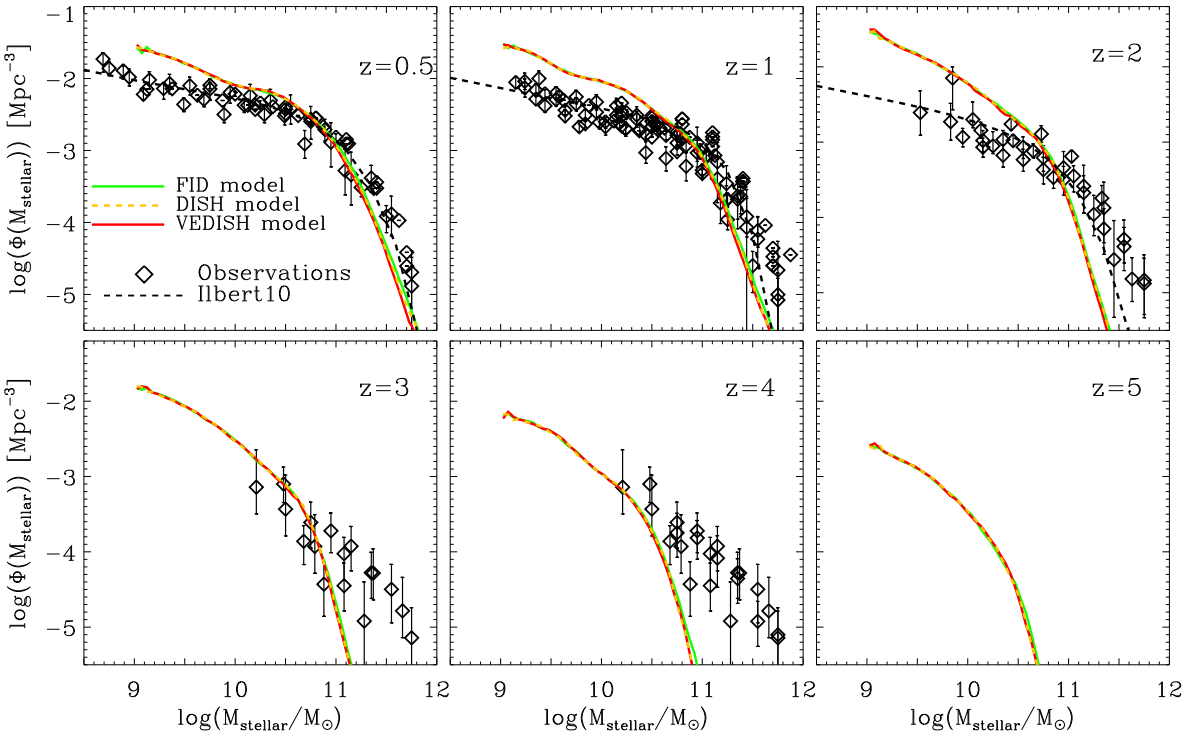

Figure 2. Redshift evolution of the stellar mass function ($z = 0.5, 1, 2, 3, 4, 5$). The solid lines show the FID (green) and the VEDISH (red) model and the orange dashed lines the DISH model. The black dashed lines depict observations from Ilbert et al. (2010) and the symbols correspond to observations from a set of observational studies (Pérez-González et al. (2008); Bundy et al. (2005); Drory et al. (2004); Fontana et al. (2006); Marchesini et al. (2007)). **As in most SAMs, the number of low mass galaxies is overestimated (at all redshifts), while the number of high mass galaxies is underestimated at high z.**

overcomes the seed black hole masses by orders of magnitude. This trend is even more pronounced in the model of Fanidakis et al. (2010), as they allow the black holes to accrete at super-Eddington rates: e.g. at redshift $z = 6$, black holes with $M_\bullet = 10^6 M_\odot$ have a number density of $\log \Phi = -2.7$ Mpc^{-3} dex^{-1}, whereas we obtain a number density of only $\log \Phi = -4$ Mpc^{-3} dex^{-1} in the VEDISH model.

The evolution of the active fraction of black holes is shown in Fig. 4. The three panels correspond to the different models (FID: upper panel, DISH: middel panel and VEDISH: lower panel), where colored lines illustrate the model results at different redshifts ($z = 0, 0.5, 1, 2, 3, 4, 5, 6$). We consider only AGN with bolometric luminosity larger than $10^{43.5}$ erg/s. The grey symbols show the local observations. We find that the evolution of the active black hole fraction varies from model to model, implying that our modifications to the recipes for BH formation and evolution have a significant influence on the active fraction at all redshifts. Comparing the DISH model with the FID model we can see two effects: At high redshifts $z \geqslant 3$, the number of active black holes with masses between $10^6 < M_\bullet < 10^8 M_\odot$ is greatly increased due to the heavy seeding mechanism and the large scatter in the accreted gas mass. At low redshifts $z \leqslant 1$, the number of active black holes with masses below $10^{8.3} M_\odot$ rises as a consequence of the additional gas accretion due to disk instabilities. Furthermore, as already seen in Fig. 1, the limited accretion rate in the VEDISH model reduces the fraction of AGN with massive black holes ($> 10^{8.3} M_\odot$) at $z < 0.5$.

6 NUMBER DENSITY EVOLUTION OF AGN

The different panels in Fig. 5 show the redshift evolution of the AGN number densities as a function of the bolometric luminosity, for the six different models. In this section, our SAM predictions are compared to the observational compilation from Hopkins et al. (2007). In their study, they convert the AGN luminosities from different observational data sets and thus, from different wavebands (emission lines, NIR, optical, soft and hard X-ray) into bolometric ones. They assume a luminosity dependence of the obscured fraction (the less luminous the more obscured) and the same number of Compton-thick ($N_H > 10^{24}$ cm^{-2}) and Compton-thin (10^{23} cm$^{-2} < N_H < 10^{24}$ cm^{-2}) AGN. However, there are many aspects of the obscuration corrections that are still being vigorously debated. Some recent studies suggest that the obscured fraction is dependent on both luminosity and redshift (Hasinger 2008; Fiore et al. 2012), in contrast with the non-redshift dependent model of Hopkins et al. (2007). There are also uncertainties surrounding the dust correction for the UV luminosity; Hopkins et al. (2007) compute the amount of dust (and therefore extinction), by adopting an N_H distribution from X-ray observations, and a Galactic dust-to-gas ratio. However, it has been shown that AGN absorbers do not have a Galactic dust to gas ratio

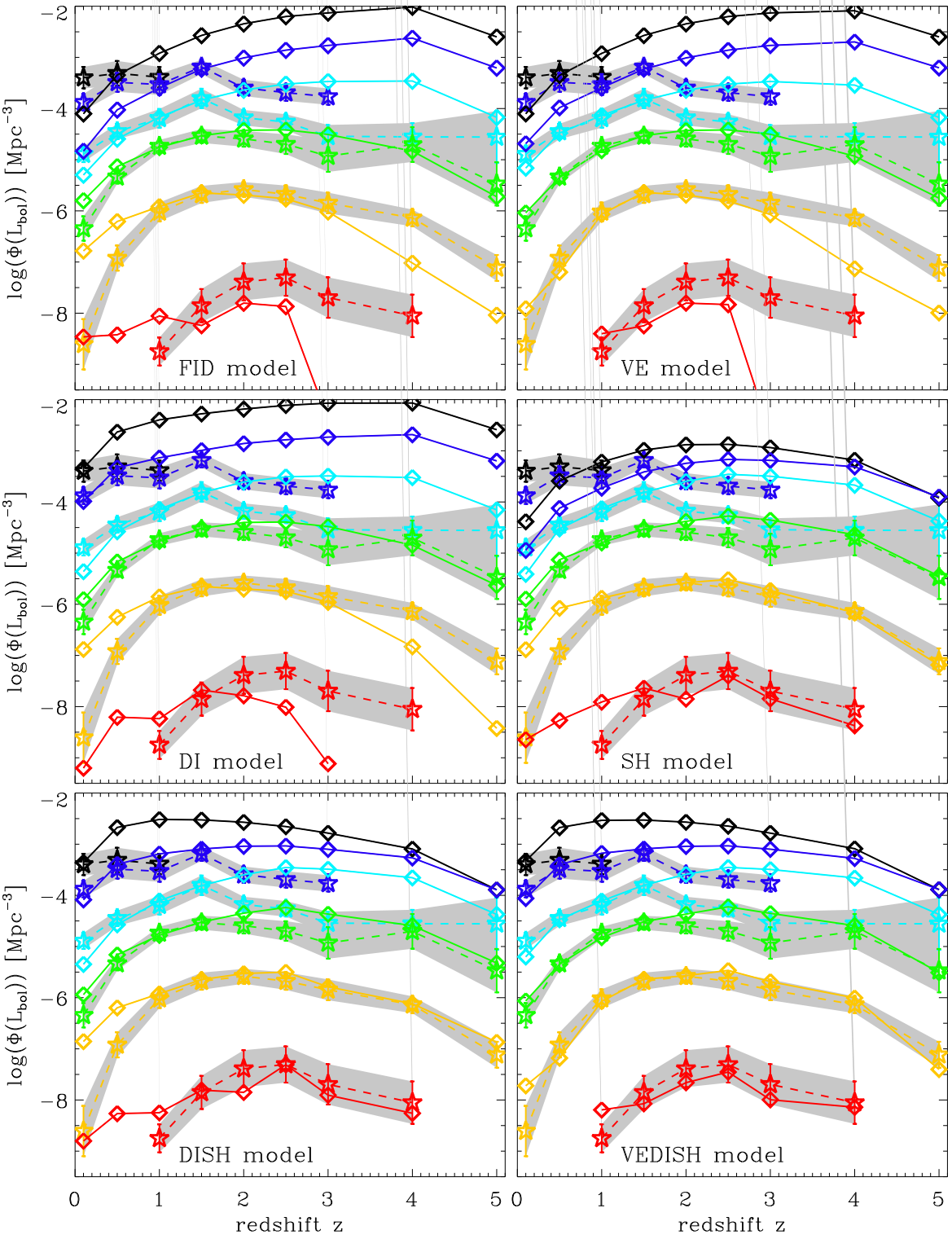

Figure 5. Number densities of AGN versus redshift for the six different SAM models (FID, VE, DI, SH, DISH and VEDISH) as indicated in the legend. Different colors illustrate different bolometric luminosity bins: red: $47.5 < \log(L_{\rm bol})$, yellow: $46.5 < \log(L_{\rm bol}) < 47.5$, green: $45.5 < \log(L_{\rm bol}) < 46.5$, light blue: $44.5 < \log(L_{\rm bol}) < 45.5$, dark blue: $43.5 < \log(L_{\rm bol}) < 44.5$, black: $42.5 < \log(L_{\rm bol}) < 43.5$. Solid lines and open squares show the corresponding model predictions; dashed lines and stars together with grey shaded areas indicate the observational compilation from Hopkins et al. (2007). While the FID model shows the opposite of "downsizing" behavior, with luminous objects forming late and low-luminosity objects forming early, we obtain a fairly good match to the observations for the VEDISH model.

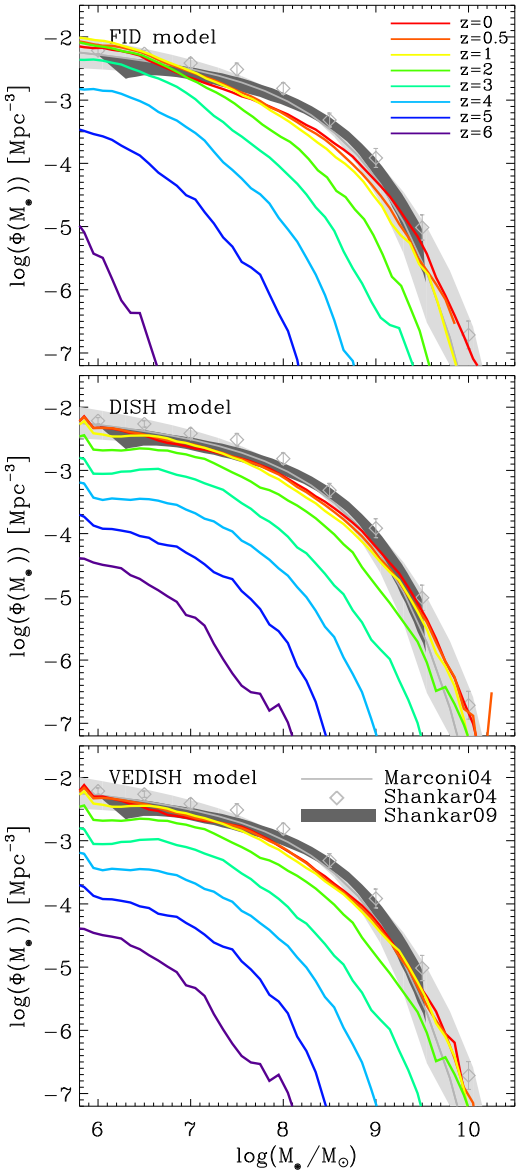

Figure 3. Redshift evolution of the black hole mass function. The colored lines illustrate the SAM results of the FID (upper panel), DISH (middle panel) and the VEDISH (low panel) model at different redshifts. The grey lines and symbols correspond to observational estimates (Marconi et al. 2004; Shankar et al. 2004, 2009) at $z = 0$. Massive black hole seeds significantly increase the number of black holes with masses between $10^6 < M_\bullet < 10^8 M_\odot$ at $z > 4$.

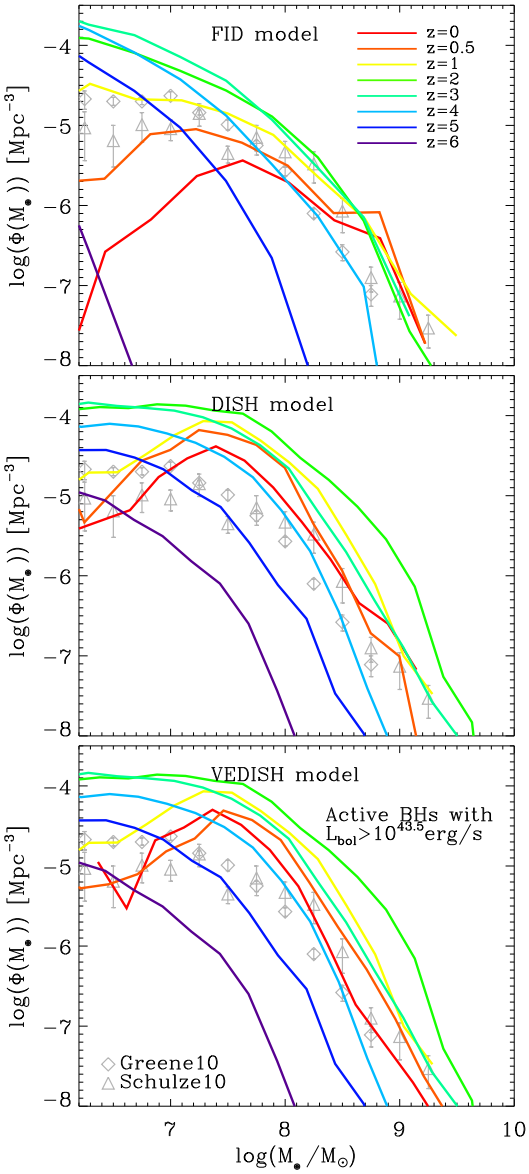

Figure 4. Redshift evolution of the black hole mass function of active black holes with bolometric luminosities larger than $L_{\rm bol} > 10^{43.5}$ erg/s. Colored lines illustrate the SAM results of the FID (upper panel), the DISH (middle panel) and the VEDISH (lower panel) model at different redshifts. For comparison, the grey symbols illustrate observations of the active black hole mass function at $z = 0$ (Greene et al. 2010; Schulze & Wisotzki 2010). Massive seeds increase the number of active black holes at high redshift and disk instabilities increase the number of active low mass black holes at low redshift.

(Maiolino et al. 2001, 2004). The result is that they probably over-estimate the extinction, which might result in slightly higher luminosities for the optically selected quasars (F. Fiore, personal communication). Because of these uncertainties, we both compare the obscuration-corrected observational compilation of Hopkins et al. (2007) with our unobscured model predictions, and in Section 7.2 we attempt to correct our model predictions for obscuration and compare with recent soft and hard X-ray measurements of the AGN luminosity function.

The upper left panel in Fig. 5 shows the FID model. The number densities at the peak of each luminosity bin are in quantitative agreement with the observations implying that the FID model reproduces the correct order of magnitude of AGN number densities in the different luminosity bins. However, the observed time evolution of the peaks of the different luminosity classes are not correctly predicted by the FID model, which shows the typical "hierarchical" behavior in which the number of low-luminosity objects peaks earlier

than the number density of higher luminosity objects. We can summarize this problem more quantitatively as follows:

- $z < 2$: over-prediction of AGN with $\log(L_{\rm bol}) > 46$
- $z < 2$: under-prediction of AGN with $\log(L_{\rm bol}) < 46$
- $z > 3$: under-prediction of AGN with $\log(L_{\rm bol}) > 46$
- $z > 3$: over-prediction of AGN with $\log(L_{\rm bol}) < 45$

As the fiducial model reproduces the black hole mass function at z=0, we can assume that there are the correct number of black holes. Therefore the first point suggests that at low redshifts either too high a fraction of massive black hole are accreting or these massive black holes are accreting at rates that are too high. Moreover, assuming that activity is triggered by merger events implies that the natural decrease in the major merger rate is not sufficient to produce the observed steep decline in the AGN number densities. It has been shown that the galaxy merger rate predicted by the S08 models matches observations (Jogee et al. 2008, Lotz et al. 2011) so this is not likely to be the cause of the discrepancy. The low number densities of moderately luminous AGN may indicate, however, that the AGN activity might not only be triggered by merger events, but also by secular evolution processes. The deviations at high redshift may be a consequence of massive black holes forming too late in the SAM as well as possibly the non-redshift-dependent dust obscuration correction. The excess of moderate and low luminosity AGN at high redshift may be partly due to the similar over-prediction of low-mass galaxies in the SAM, which we already discussed in Section 5.

We experimented with whether we could achieve better reproduction of the observed downsizing of BH activity by just modifying the values of some free parameters in the FID SAM, without changing any physical ingredients. For example, we tested the effect of varying the strength of Supernova and radio-mode feedback (as suggested in Fontanot et al. 2006). We find that for stronger supernova feedback (doubling the normalization of the mass loading factor for SN-driven winds $\epsilon^0_{\rm SN}$) we achieve a decrease in the number density of AGN at *all* redshifts, resulting in overall a worse match to the observations. Even if the number density of moderately luminous objects ($L_{\rm bol} < 10^{45}$ erg/s) at high redshifts decreases (towards the observational data), this is not sufficient to achieve a reasonably good match to observations in this range. Increasing the strength of the radio-mode feedback reduces the number of luminous AGN ($L_{\rm bol} > 10^{45}$ erg/s) between redshifts $0 < z < 4$, again resulting in worse agreement with the observational compilation than for the FID model itself. If we assume 'halo quenching' instead of the radio-mode feedback model, i.e. no cooling is allowed above a certain threshold halo mass ($M_{\rm halo,thres} = 10^{12} M_\odot$), we obtain a decrease of the number of luminous AGN, but again at *all* redshifts, and not redshift dependent as observed. To increase the number density of moderately luminous objects at low redshifts, we varied the timescale (t_Q) in the power-law decline phase of a quasar episode. A study by Marulli et al. (2008) has shown that a power-law decline growth phase in their quasar mode *does* increase the number density of moderately luminous AGN at low redshift, resulting in a better agreement with the observations. However, within our study it is found that varying t_Q is not sufficient to match the observations. Therefore, we can conclude that downsizing cannot be reproduced solely by varying the free parameter values of our FID model. Instead, we now present the influence of the additional modifications for black hole formation and growth as outlined in Section 3.

The result for the VE model (i.e. assuming a sub-Eddington accretion limit dependent on the cold gas fraction) is illustrated in the upper right panel of Fig. 5. For bolometric luminosities larger than 10^{46} erg/s, the cold gas fraction dependent sub-Eddington limit clearly reduces the number density of AGN. We find that we are able to reproduce the observed steep decline in the number densities of bright AGN at $z < 2$ reasonably well in this way. This supports the idea that the cold gas content of a galaxy may regulate the efficiency of black hole accretion, in particular the maximum accretion rate that can be reached in a merger. We may speculate that low cold gas densities lead to smaller viscosities so that it takes longer for the gas to lose its angular momentum and thus, to be accreted onto the black hole. Our results imply that even when massive black holes experience major mergers, if the gas fractions in their host galaxies are low they may not produce luminous AGN because they never accrete at close to the Eddington rate.

The middle left panel of Fig. 5 shows the results of the DI model, assuming an additional BH accretion mode due to disk instabilities. For a luminosity range of $43 < \log(L_{\rm bol}) < 45$, the number of AGN is increased, resulting in a reasonably good match with the observational compilation for $z < 1.5$. For the lowest luminosity bin, however, the number of AGN is now over-predicted. Nevertheless, this additional accretion mechanism seems to play an important role for triggering the activity of faint AGN. In strong contrast to our model, black hole accretion due to disk instabilities in the Galform-model (e.g. Fanidakis et al. 2010) provides the *major* contribution to AGN number densities for *all* luminosities and at *all* redshifts. In the Munich-models as presented by Marulli et al. (2008) and Bonoli et al. (2009), black hole accretion due to disk instabilities is not accounted for at all, but they still slightly under-predict the number of moderately luminous AGN, even in their best-fit model. This further supports the need for BH accretion driven by secular evolution processes, in addition to mergers.

The effect of a heavy seeding mechanism together with a halo mass limit for black hole formation (SH model) is illustrated in the middle right panel of Fig. 5. The number of bright AGN at high redshift is increased and can match the observational data. This is a consequence of large seed black hole masses and a large scatter in the accreted gas mass. As we cap BH growth at the Eddington rate, having more massive seeds means that these early black holes can grow faster, leading to a larger number of massive and active black holes at early times than in the FID, VE and DI models. Our result indicates that black holes probably have to undergo a phase of very rapid growth at high redshifts ($z > 5$), even if it is still unknown whether and how such massive seed black holes can form out of direct core-collapse or whether less massive seeds have to accrete at super-Eddington rates. However, we find that assuming even more massive black hole seeds with masses of $M_{\bullet,\rm seed} = 10^6 M_\odot$ results too few moderately luminous AGN at high redshift ($z \approx 5$) in our model. The halo mass limit for seed black hole formation also reduces the number density of faint AGN, as black holes in

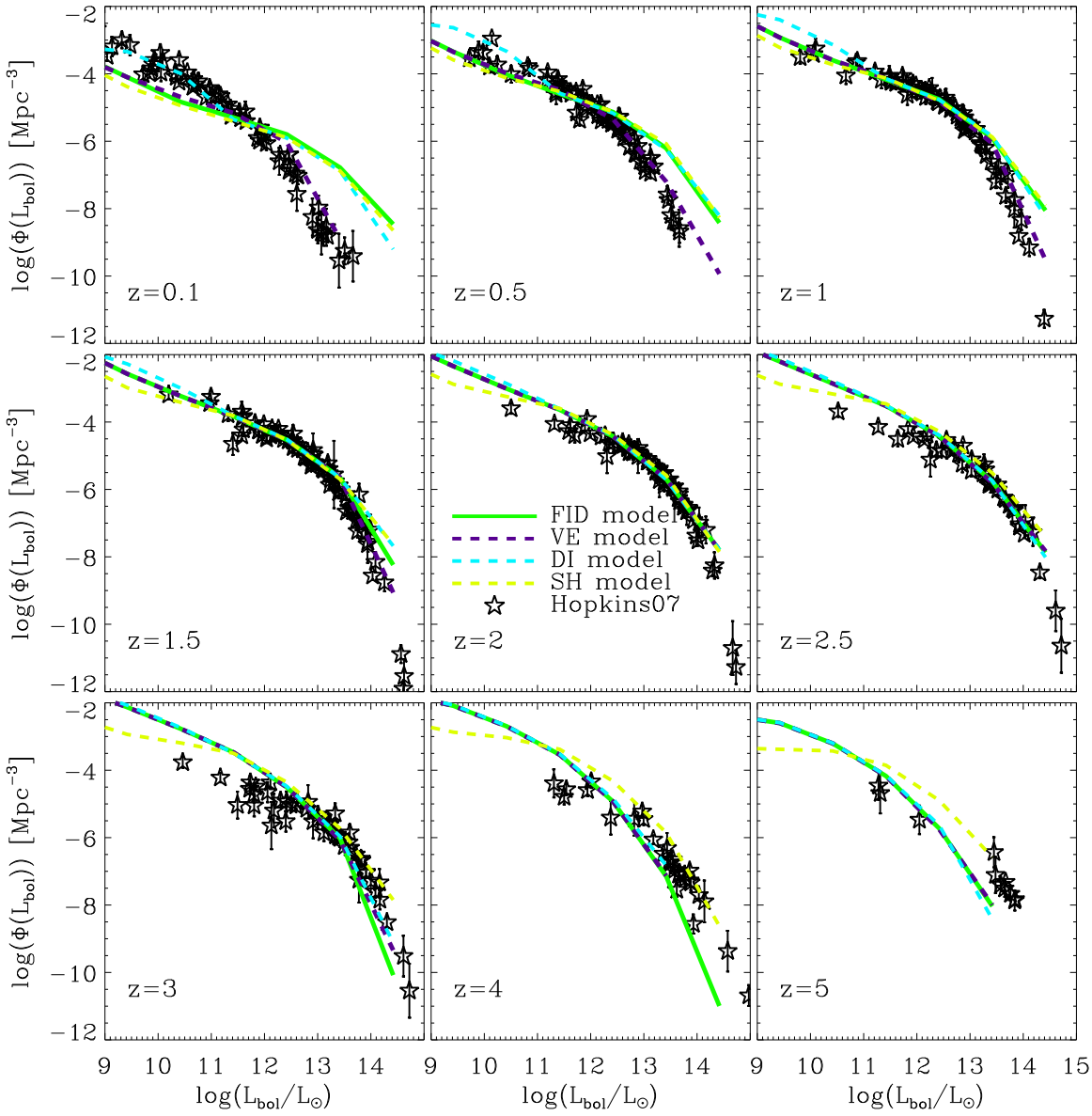

Figure 6. Bolometric quasar luminosity functions at different redshifts. Black stars show the observational compilation of Hopkins et al. (2007). The green solid lines correspond to the output of the FID model, the purple, dashed lines show the VE model, the light blue, dashed lines the DI model and the dark blue, dashed lines the SH model.

low-mass halos are not allowed to form and to accrete gas. However, even if this second effect results in better agreement with the observational data, it does not seem to be fully sufficient for reproducing them. This might indicate that the dependence of seed mass on halo mass is more complex than we have assumed in this simple model, or might be be due to redshift-dependent obscuration, which has not been accounted for in the observational comparison that we are using here (see Section 7.2).

Finally, the combination of the individual modifications which have been discussed so far is presented by the DISH and the VEDISH model (lower left and lower right panel of Fig. 5). We find that the changes in the AGN number densities seen for the individual modifications sum in a straightforward way, without significantly influencing each other. Thus, the VEDISH (="best-fit") model is able to reproduce the observed downsizing trend fairly well, and can predict the *correct time-evolution* of the peaks of the luminosity dependent number density curves. However, even in our best-fit model, the number of faint AGN is still over-predicted at redshifts between $4 > z > 2$. This might be due to the difficulty of detecting these objects at high redshifts, either because they may not be easily recognizable as AGN, or because of obscuration.

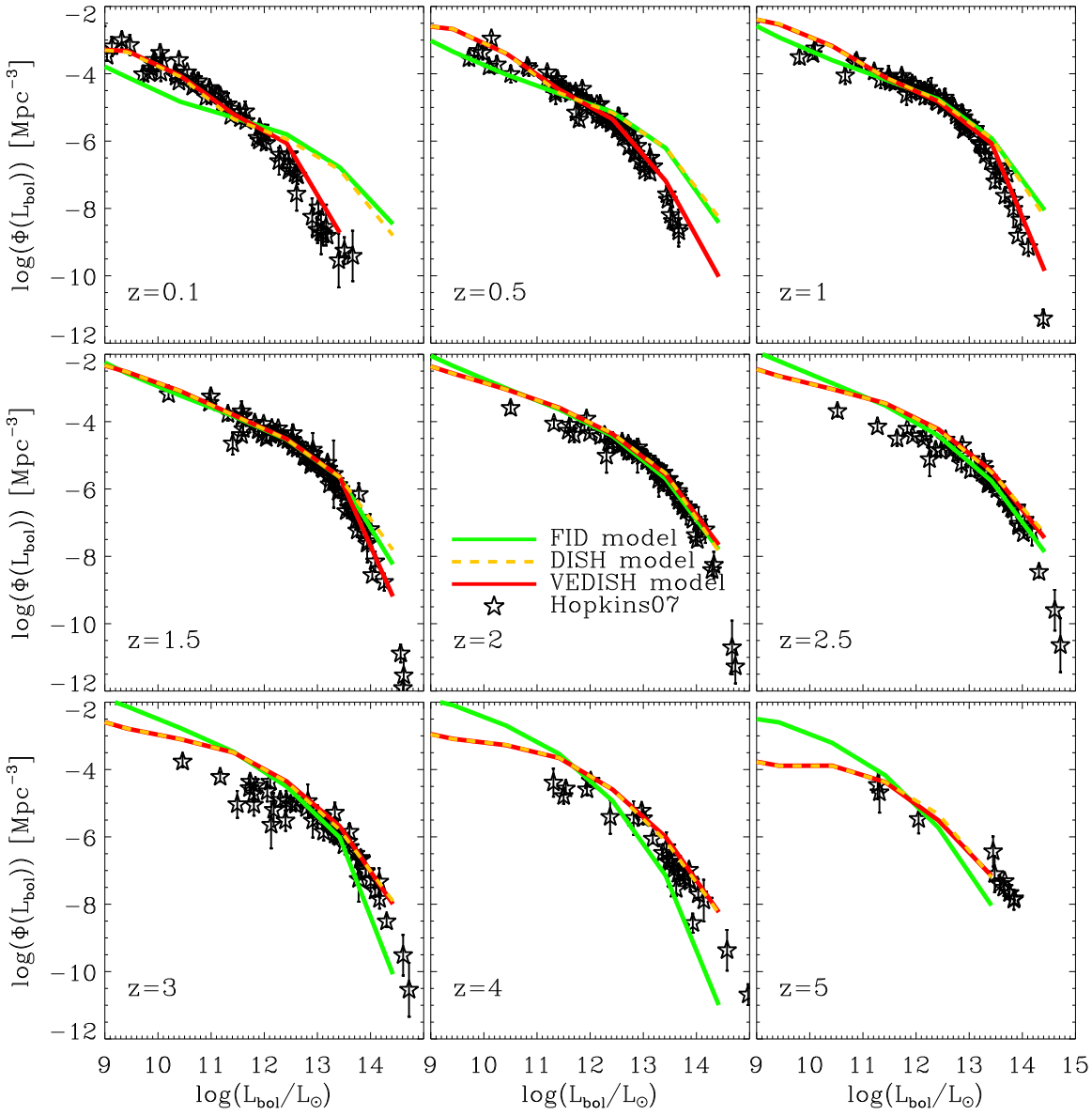

Figure 7. The same as in Fig. 6, but for different SAM models: the green solid lines correspond to the output of the FID model, the orange, dashed lines show the DISH model and the red, solid lines illustrate the results from the VEDISH model. For the VEDISH model, a reasonably good agreement with observations is obtained.

7 THE AGN LUMINOSITY FUNCTION

7.1 Bolometric luminosities

The effects of our individual modifications for black hole growth and the final success of the VEDISH model can also be explicitly seen in Figs. 6 and 7, where the bolometric AGN luminosity function (AGN LF) is plotted at different redshifts, and again compared with the observational compilation from Hopkins et al. (2007). Fig. 6 shows that the DI model raises the low-luminosity end by about one order of magnitude in AGN number densities, while the VE models lowers the high-luminosity end by more than two orders of magnitude at $z \leqslant 1.5$. The SH model changes the AGN number densities at $z \geqslant 3$ by lowering the low-luminosity end and raising the high-luminosity end, each of them by about one order of magnitude. The cumulative effect of the separate alterations is shown by the DISH and the VEDISH model (Fig. 7). While the DISH model still fails to reproduce the high luminosity end at low redshift, the VEDISH model represents a fairly good match with the observational data for the whole redshift range.

7.2 X-ray Luminosity Functions

We now compare our model predictions with recent observational determinations of the AGN LF in the hard and soft X-ray bands (Hasinger et al. 2005; Ebrero et al. 2009; Aird et al. 2010; Fiore et al. 2012). In contrast to the previ-

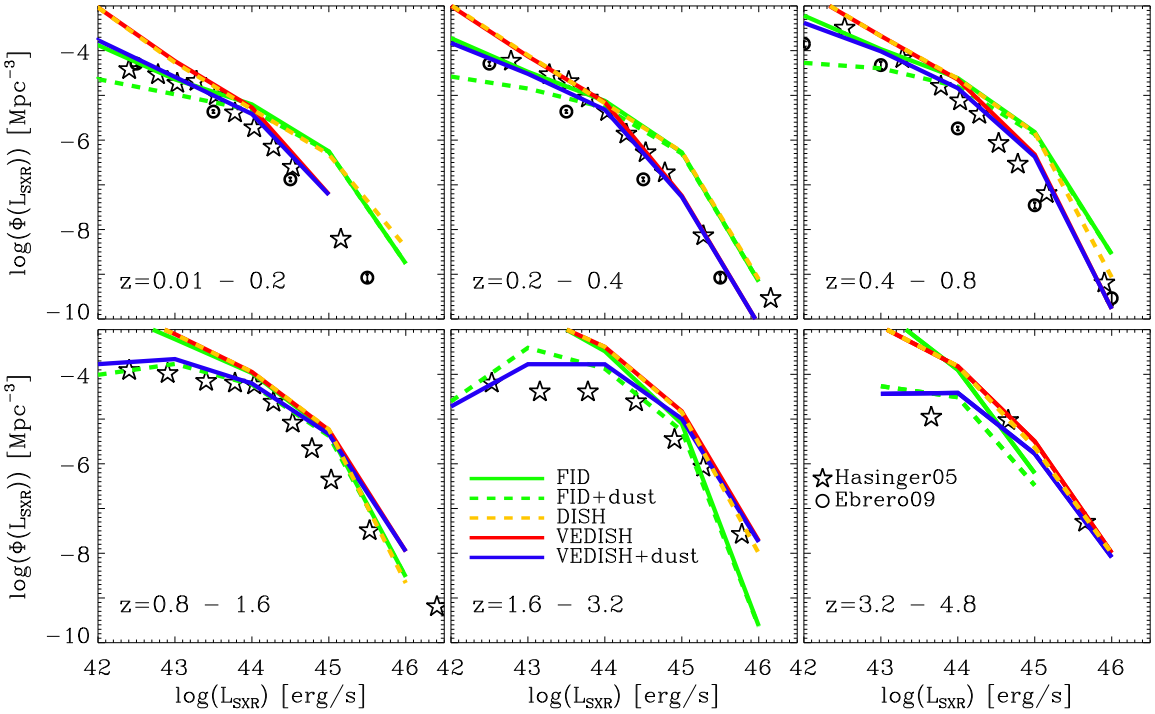

Figure 8. Soft X-ray AGN luminosity function for different redshift ranges. Black stars and circles show the observational data from Hasinger et al. (2005) and Ebrero et al. (2009), respectively. The solid green, dashed orange and solid red lines correspond to the results of the FID, the DISH and the VEDISH model and the blue solid lines illustrate the results of the VEDISH model with an obscuration correction according to Hasinger (2008). The VEDISH model including the obscuration correction is in fair agreement with the observational data.

ous section, we do not attempt to correct the observations for obscuration, but instead apply an obscuration correction to our models. We convert the modeled, bolometric luminosities into hard and soft X-ray luminosities ($0.5-2$ keV and >2 keV) using the bolometric correction according to Marconi et al. (2004). In their study, the hard and soft X-ray luminosities $L_{\rm HXR}, L_{\rm SXR}$ are approximated by the following third-degree polynomial fits:

$$\log(L_{\rm HXR}/L_{\rm bol}) = -1.54 - 0.24\mathcal{L} - 0.012\mathcal{L}^2 + 0.0015\mathcal{L}^3 \quad (14)$$

$$\log(L_{\rm SXR}/L_{\rm bol}) = -1.65 - 0.22\mathcal{L} - 0.012\mathcal{L}^2 + 0.0015\mathcal{L}^3 \quad (15)$$

with $\mathcal{L} = \log(L_{\rm bol}/L_{\odot}) - 12$. These corrections are derived from template spectra, which are truncated at $\lambda > 1\ \mu m$ in order to remove the IR bump and which are assumed to be independent of redshift (therefore the resulting bolometric corrections are also assumed to be redshift independent). Additionally, we apply a correction for obscuration to the model luminosities, as suggested by several observational studies (Ueda et al. 2003; Hasinger 2004; La Franca et al. 2005), in which it has been shown that the fraction of obscured AGN is luminosity dependent and decreases with increasing luminosity. While older studies such as Ueda et al. (2003) and Steffen et al. (2003) did not find a clear dependence of obscuration on redshift, several recent observational studies (Ballantyne et al. 2006; Gilli et al. 2007; Hasinger 2008) propose a strong evolution of the obscured AGN population (with the relative fraction of obscured AGN increasing with increasing redshift). Here, we follow the study of Hasinger (2008), where they compare the same AGN in both the soft and hard X-ray band so that they can derive an approximation for the obscured fraction in the soft X-ray band. The obscured fraction is then given by this equation:

$$f_{\rm obsc} = -0.281(\log(L_{\rm LXR}) - 43.5) + 0.279(1+z)^{\alpha}. \quad (16)$$

where they find that a value of $\alpha = 0.62$ provides the best fit to their observational data. By calculating the obscured fraction of AGN in the soft X-ray band, we can model the visible fraction of AGN $f_{\rm vis} = 1 - f_{\rm obsc}$ and thus, the visible number density of AGN in the soft X-ray range is given by:

$$\Phi_{\rm vis}(L_{\rm SXR}) = f_{\rm vis} \times \Phi_{\rm total}(L_{\rm SXR}) \quad (17)$$

Fig. 8 shows the *soft* X-ray luminosity function for different redshift ranges predicted by our FID, DISH and VEDISH models, compared with observations from Hasinger et al. (2005) and Ebrero et al. (2009). We show the model predictions with and without the obscuration correction described above. For the high-luminosity end ($L_{\rm SXR} > 10^{45}$ erg/s), obscuration does not influence our results and thus, one can see the same trends as already discussed in Fig. 7. Turning to the low-luminosity end at low redshifts ($z \leqslant 0.8$), the FID model matches the observational data, while the DISH and VEDISH model overproduce the number density of AGN. However, considering obscuration effects leads to better agreement of the VEDISH model with the observed number densities than the FID model. At high redshift ($z > 0.8$), both the FID and the VEDISH model over-predict the number of moderately luminous AGN by almost the same amount, and both models including obscu-

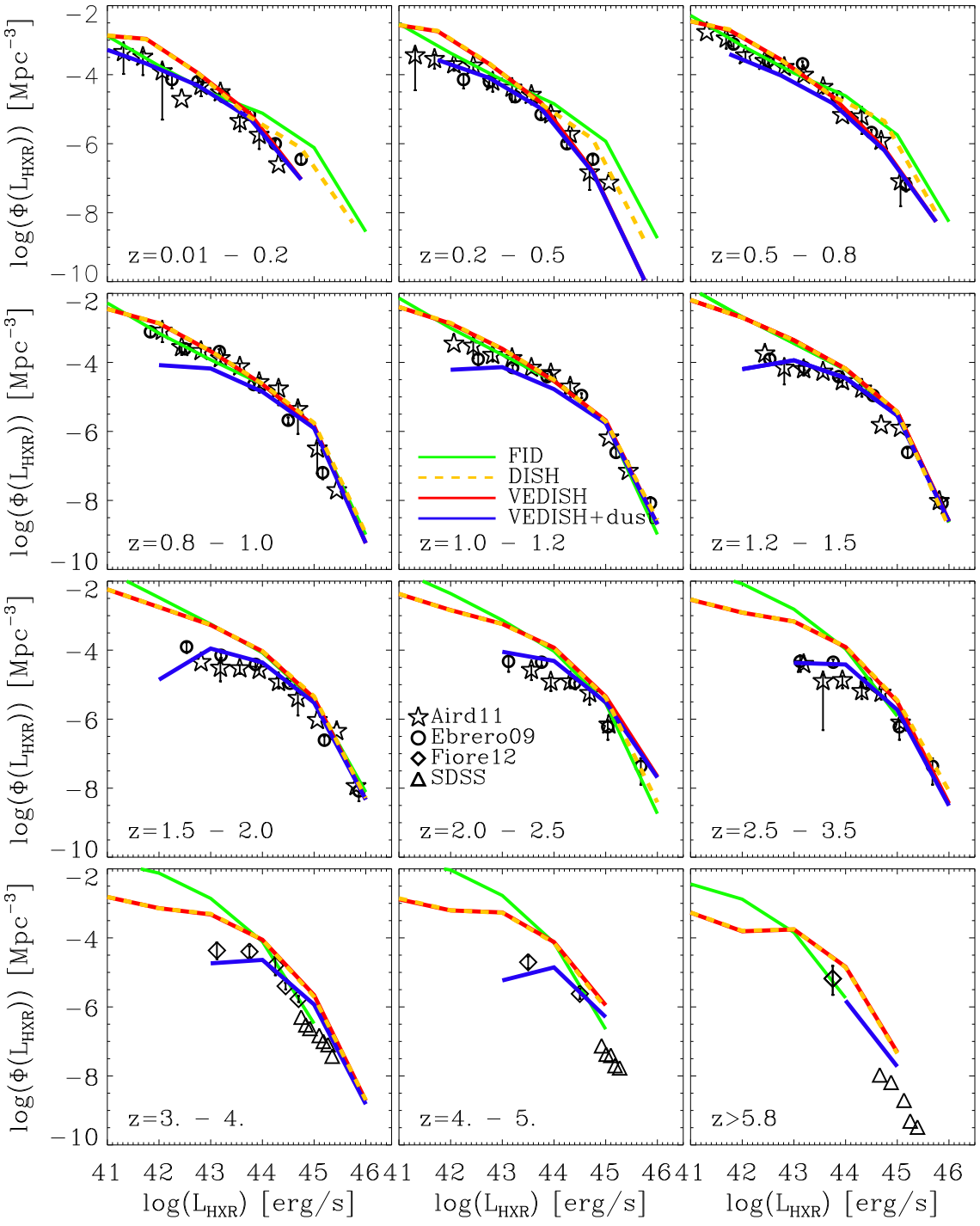

Figure 9. Hard X-ray AGN luminosity function for different redshift ranges. Black symbols show the observational data of Ebrero et al. (2009); Aird et al. (2010); Fiore et al. (2012) and data from the SDSS (optical luminosity is converted into X-ray luminosity as in Fiore et al. (2012)). The solid green, dashed orange and solid red lines illustrate the output of the FID, the DISH and the VEDISH model. The blue solid lines illustrate the results of the VEDISH model with an obscuration correction according to Hasinger (2008). The latter is able to predict the observed hard X-ray LF reasonably well.

ration can achieve a fairly good agreement with the observations. Overall, the VEDISH model including AGN obscuration can predict the observed soft X-ray luminosity function reasonably well, supporting the adoption of a redshift-dependent obscured fraction. Fanidakis et al. (2010) use the same bolometric conversion for calculating soft X-ray luminosities and the same dust obscuration correction as in our study. They show that they are able to match the soft X-ray luminosity functions from the observational study of Hasinger et al. (2005) as well.

Fig. 9 illustrates the *hard* X-ray luminosity functions predicted by our models for different redshift ranges, compared with observational data (Ebrero et al. 2009, Aird et al. 2010, Fiore et al. 2012, Fiore et al. 2012). The VEDISH model is able to reproduce the high-luminosity end pretty well, whereas it over-predicts the number of AGN at the low-luminosity end at all redshifts (with a larger discrepancy at higher redshift). One possible explanation might be again due to obscuration as even $2-10$ keV X-ray surveys might miss a significant fraction of moderately obscured AGN (25% at $N_H = 10^{23}$ cm^{-2}) and nearly all Compton-thick AGN ($N_H > 10^{24}$ cm^{-2}, Treister et al. 2004; Ballantyne et al. 2006). From fits to the cosmic X-ray background, Gilli et al. (2007) predict that both moderately obscured and Compton-thick AGN are as numerous as unobscured AGN at luminosities higher than $\log(L_{0.5-2\mathrm{keV}}) > 43.5$[ergs/s], and four times as numerous as unobscured AGN at lower luminosities ($\log(L_{0.5-2\mathrm{keV}}) < 43.5$[ergs/s]). For this reason, we made the very simplified assumption that the fraction of obscured AGN in the hard X-ray band is the same as in the soft X-ray band. This results in a fairly good match to the observed low-luminosity end at all redshifts, except around $z \sim 1$ where the obscuration-corrected model under-predicts the number of faint AGN. Therefore, our model results are consistent with the existence of an obscured fraction of AGN in the hard X-ray band (Compton-thick AGN) that is of the same order of magnitude as the obscured fraction in the soft X-ray band. Interestingly, Fanidakis et al. (2010) show that they are able to match the hard X-ray luminosity functions from an observational study of Ueda et al. (2003) *without* including any obscuration effects. However, their predictions are only illustrated for a comparatively small redshift range of $0.2 < z < 1.6$ and for hard X-ray luminosities larger than $L_{\mathrm{HXR}} > 10^{42}$ erg/s, where our unobscured VEDISH model predictions are also in good agreement with the observational data.

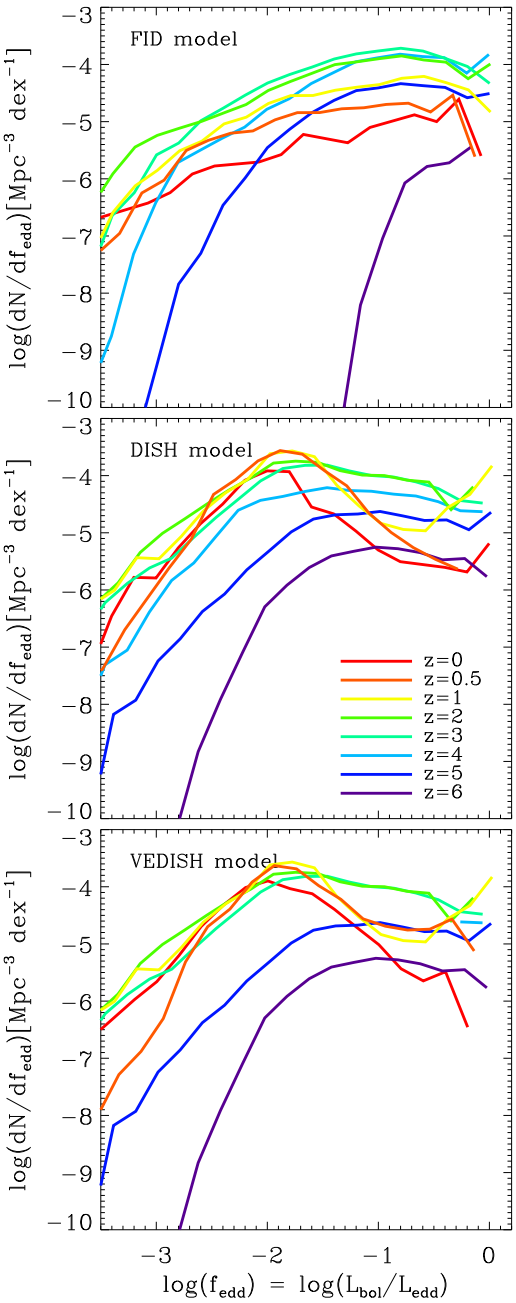

Figure 10. Eddington ratio distributions for the FID, DISH and the VEDISH models (upper, middle and lower panel panel, respectively). Different colors correspond to different redshifts ($z = 0.5, 1, 2, 3, 4, 5, 6$). Note that here we show only accreting black holes with bolometric luminosities larger than 10^{43} erg/s. The modifications in the VEDISH model cause the peaks of the distributions to shift towards smaller Eddington ratios with time, in qualitative agreement with observational studies (Vestergaard 2003; Kollmeier et al. 2006; Kelly et al. 2010; Schulze & Wisotzki 2010)

8 EDDINGTON RATIO DISTRIBUTIONS

Having assessed our models by comparing with the observed AGN LF, we now examine the consequences of our modifications of the black hole growth prescriptions on the Eddington ratio distribution and on the AGN luminosity-black hole mass plane. In Fig. 10 we show the redshift evolution of the Eddington ratio distributions for the FID (upper panel), the DISH (middle panel) and the VEDISH model (lower panel). Different colors indicate different redshift steps ($z = 0, 0.5, 1, 2, 3, 4, 5, 6$). Consistent with our previous investigation, and typical limits of observational samples, we consider only AGN with bolometric luminosities larger than 10^{43} erg/s. In all models, the fraction of

AGN that are are accreting at smaller Eddington ratios increases strongly with decreasing redshift. This is because at later times, black holes spend less of their time in the first regime, i.e. accreting at the Eddington rate, but mainly reside in the second regime, the power-law decline dominated "blowout" accretion phase. These black holes are relics from an earlier, more active phase with higher accretion rates. While, however, in the FID model the Eddington ratios are still peaking between $f_{\rm edd} = 0.1 - 1$ at *all* redshifts, in the DISH and the VEDISH models the peaks of the distribution curves are clearly shifted towards smaller Eddington ratios with decreasing redshift. This is mainly caused by the additional black hole accretion due to secular evolution processes. At $z = 6$ the distributions of the DISH and VEDISH models peak at $f_{\rm edd} \approx 0.1$, while at $z = 0$ the peaks are located around $f_{\rm edd} \approx 0.01$. Thus, the majority of AGN at $z = 0$ are not radiating at or near the Eddington limit anymore, which is in qualitative agreement with observational studies (Vestergaard 2003; Kollmeier et al. 2006; Kelly et al. 2010; Schulze & Wisotzki 2010). For example, Kelly et al. 2010 find that the Eddington ratio distribution (using broad-line quasars between $z = 1 - 4$) peaks at an Eddington ratio of $f_{\rm edd} = 0.05$. Furthermore, the large seed black hole masses and the large scatter in the accreted gas mass in the DISH and VEDISH models lead to a significantly larger number of accreting black holes with Eddington ratios between $0.01 < f_{\rm edd} < 1$ at $z > 4$ than in the FID model. Finally, the VEDISH model additionally shows that as a consequence of the sub-Eddington accretion rate limit (dependent on the cold gas fraction), the number of black holes accreting close to the Eddington limit at $z = 0$ is reduced by about one order of magnitude compared to the DISH model. Altogether, we find that the downsizing behavior seems to imply that the peaks of the Eddington ratio distributions are shifted towards smaller Eddington ratios with decreasing redshift, and the number of black holes accreting close to the Eddington-rate is low at $z = 0$ ($\log(dN/df_{\rm edd}) = -6.5$ Mpc^{-3} dex^{-1}), while at high redshifts a large number of black holes ($\log(dN/df_{\rm edd}) = -5.2$ Mpc^{-3} dex^{-1}) are accreting within a broad range of Eddington ratios $0.01 < f_{\rm edd} < 1$.

9 LUMINOSITY-BLACK HOLE MASS-PLANE

Fig. 11 shows the bolometric AGN luminosity-black hole mass-plane at $z = 0$ (left column), $z = 2$ (middle column) and $z = 5$ (right column) for different SAMs (first row: FID model, second row: VE model, third row: DISH model and fourth row: VEDISH model). The circles in each panel correspond to our model AGN with a bolometric luminosity cut of $L_{\rm bol} > 10^{43}$ erg/s and they are color coded according to their bolometric luminosity as defined in Fig. 5. We also show lines indicating accretion at the Eddington rate, an Eddington ratio of $f_{\rm edd} = 0.1$ and an Eddington ratio of $f_{\rm edd} = 0.01$. In addition, we show the observational limit in the $L_{\rm bol} - M_\bullet$-plane according to Steinhardt & Elvis (2010).

At $z = 5$ (right column of Fig. 11), in the FID and VE models, black holes within a mass range of $10^{4.7} < M_\bullet < 10^8 M_\odot$ are active, where the luminosity is almost linearly correlated with black hole mass, indicating accretion at or very close to the Eddington rate. As a consequence of the heavy seeding mechnism and of the halo mass limit for black hole formation, the mass range of active black holes is shifted towards larger values $10^{5.5} < M_\bullet < 10^{9.5} M_\odot$ in the DISH and the VEDISH models. As we showed previously, in order to reproduce the observed downsizing trend these bright AGN ($L_{\rm bol} > 10^{46.5}$ erg/s) need to appear already at these early times. Turning to $z = 2$ (middle column of Fig. 11), we see that in all models the number of AGN with massive BH ($M_\bullet > 10^9 M_\odot$) has increased relative to $z = 5$. Compared to the accretion limit of Steinhardt & Elvis (2010), all of our model results are in acceptable agreement, although we predict some massive BH accreting at or very close to the Eddington rate which strictly speaking are not 'allowed' according to the Steinhardt & Elvis (2010) results. Also for all models, the relation between black hole mass and bolometric luminosity becomes much broader — black holes with masses $M_\bullet \approx 10^8 M_\odot$ can now also power moderately luminous AGN with $L_{\rm bol} \approx 10^{43}$erg/s as they are accreting with Eddington ratios below $f_{\rm edd} < 0.01$. The probability for black holes with $M_\bullet > 10^7 M_\odot$ to accrete at Eddington ratios below $f_{\rm edd} = 0.01$ is even higher than to accrete at larger Eddington ratios. This is due to the power-law decline accretion phase that black holes are experiencing: massive black holes powering moderately luminous AGN are remnants of former, high-luminous AGN. In the DISH and VEDISH models, we can additionally see the effect of black hole accretion due to disk instabilities: the number of AGN with black hole masses of $10^7 M_\odot < M_\bullet < 10^8 M_\odot$ and with luminosities between $10^{43} < L_{\rm bol} < 10^{45}$ erg/s is significantly increased, accreting with Eddington ratios around $f_{\rm edd} \approx 0.01$. As Seyfert galaxies are mainly spiral galaxies with black hole masses in the range of $10^7 M_\odot < M_\bullet < 10^8 M_\odot$ and are — compared to quasars — only moderately luminous, disk instabilities seem indeed to provide one of the most important trigger mechanisms for their nuclear activity. Moreover, in the DISH and VEDISH models, no black holes below $10^{5.5} M_\odot$ are active, in contrast to the FID and the VE models. This is due to the halo mass limit for black hole formation.

Finally, at redshift $z = 0$ (left column of Fig. 11), the number of actively accreting black holes is significantly reduced compared to $z = 2$. The DISH and the VEDISH models show again the effect of the additional accretion channel due to disk instabilities, increasing the number of moderately luminous AGN, with typical black hole masses of Seyfert galaxies ($10^7 M_\odot < M_\bullet < 10^8 M_\odot$). While, however, in the FID and the DISH models, bright AGN can exist with massive black holes accreting at and close to the Eddington rate, in the VE and VEDISH models the limited accretion regulated by the cold gas fraction suppresses the appearance of these bright AGN. Compared to the observed accretion limit of Steinhardt & Elvis (2010), our results in the VE and VEDISH model are in very good agreement with the observed limit. This strongly suggests that the dependence of the accretion rates on the cold gas content might provide a possible physical origin for the observed accretion limit and thus, the reduced number of bright AGN at low redshifts.

Interestingly, in the study of Fanidakis et al. (2010), they obtain almost no evolution of their luminosity-black hole mass relation within a redshift range $0.5 < z < 2$. Black holes above $M_\bullet > 10^9 M_\odot$ always accrete below $f_{\rm edd} = 0.01$ (ADAF regime), as in our VE and VEDISH models. How-

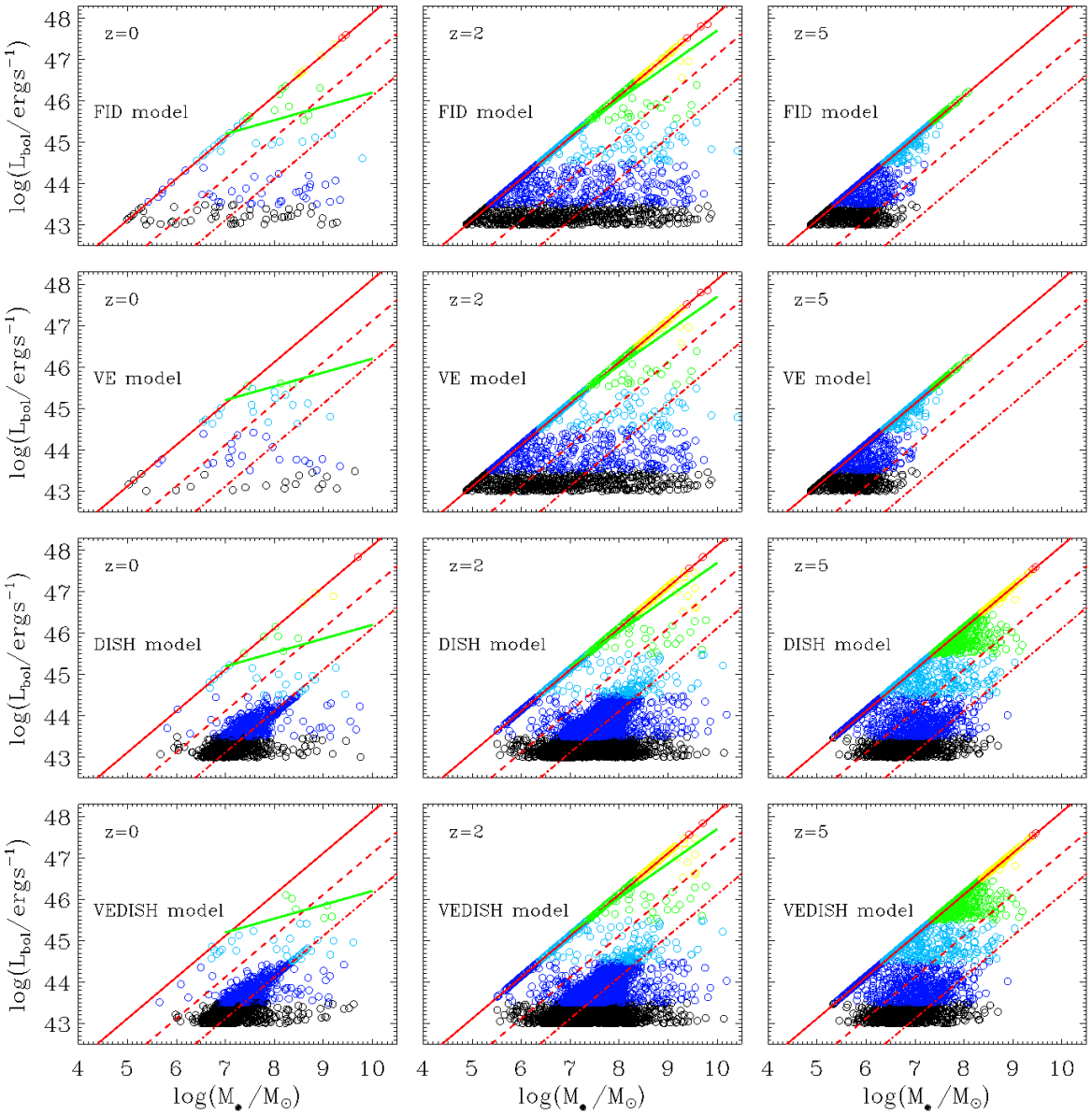

Figure 11. Bolometric luminosity versus black hole mass at $z = 0$ (left column), $z = 2$ (middle column) and $z = 5$ (right column). Different rows correspond to the FID (first row), the VE (second row), the DISH (third row) and the VEDISH (fourth row) model. The open circles illustrate actively accreting black holes at each redshift. The different colors correspond to different bolometric luminosity bins as defined in Fig. 5. The red solid lines always illustrate accretion at the Eddington rate $f_{\rm edd} = 1$, while the red dashed and dotted dashed lines depict Eddington ratios of $f_{\rm edd} = 0.1$ and $f_{\rm edd} = 0.01$, respectively. The green solid lines show the sub-Eddington limit from Steinhardt & Elvis (2010). We find that the observed upper envelope in Eddington ratio is reproduced well by our adopted gas fraction dependent accretion limit.

ever, in clear contrast to this work, in this redshift range, they still have super-Eddington accretion, in particular for black hole masses between $10^8 M_\odot < M_\bullet < 10^9 M_\odot$ (resulting in $L_{\rm bol} > 10^{46}$ erg/s). This seems to be, however, in contrast to several observational studies, such as Steinhardt & Elvis (2010), which do not find black holes with masses $M_\bullet > 10^7 M_\odot$ accreting near or at the Eddington limit at low redshifts $z = 0.2 - 0.4$.

10 SUMMARY AND DISCUSSION

In this study, we have used the semi-analytic model of S08 to study the origin of the observed anti-hierarchical behavior of BH activity within the framework of hierarchical structure formation. In the original S08 SAM (FID), all AGN are merger-driven, with the prescription for BH accretion and the light curve models based on hydrodynamic binary merger simulations. In these models, BH growth is self-regulated, resulting in a tight scaling relation between BH mass and spheroid mass. Following a merger, BH are

allowed to grow until they reach a critical mass, at which the luminosity emitted by the AGN is sufficient to power a pressure-driven outflow that is able to slow down subsequent accretion, and eventually to unbind the gas in the galaxy. In this picture, BH accrete at the Eddington limit until they reach this critical mass, after which, in the "blowout" phase, the accretion rate declines as a power law function of time. The FID model reproduces the observed number densities of AGN at $z \sim 2$ over a wide range of bolometric luminosity, but in its original form it does not reproduce the observed downsizing trend: at low redshift, the FID model overproduces the number of bright AGN and under-predicts the number of moderately luminous AGN, while at high redshift, this trend is reversed. Therefore, we extended the FID model by considering different modifications to the physical recipes for black hole growth, and investigated their effect on the AGN evolution in different luminosity bins. We summarize our main findings:

1. **A sub-Eddington limit dependent on the cold gas fraction of the host galaxy (VE model)**: The FID model overproduces luminous AGN at low redshift ($z < 1$). We found that introducing a sub-Eddington cap on the BH accretion rate which was dependent on the gas fraction of the progenitor galaxies resulted in improved agreement with the observations in this regime. In our model, the gas content of massive galaxies is strongly dependent on the Radio Mode AGN feedback, which suppresses cooling in massive halos at low redshift. Low cold gas fractions may retard the loss of angular momentum due to smaller viscosity and thus, the cold gas flow onto the central black hole may be suppressed. However, we found that we only obtained a good match to observations when we implemented this accretion rate cap at $z \leqslant 1$. Extending the same gas-fraction dependent limit to all redshifts results in too few of the brightest AGN at redshifts between $1 < z < 4$. One possible explanation might be that the evolution of the cold gas content in the FID SAM may not be correctly modeled. This could be due to incorrect or simplified cooling recipes Hirschmann et al. (2011); Lu et al. (2011) or inadequate star formation recipes (Caviglia & Somerville, in prep).
2. **An additional BH accretion triggering mechanism due to disk instabilities (DI model)**: The second main result of our study is that gas accretion onto black holes due to disk instabilities seems to be a non-negligible trigger mechanism for moderately luminous AGN with black hole masses $10^7 M_\odot < M_\bullet < 10^8 M_\odot$ at low redshift. This increases the number of AGN with bolometric luminosities 10^{43} erg/s $< L_{\rm bol} < 10^{45}$ erg/s, i.e. Seyfert galaxies, by about one order of magnitude. Our results therefore favor a 'hybrid' picture in which major merger events are the main driver of luminous AGN, especially at high redshift, while disk instabilities are the main mechanism powering moderately luminous Seyfert galaxies at low redshift (consistent with the picture suggested by e.g. Hopkins & Hernquist 2009). Note that the studies based on the Munich and the Galform model have come to rather different conclusions (see discussion below).
3. **Heavy seed black holes with a halo mass threshold for seed formation (SH model)**: Our FID model does not produce enough very luminous QSOs at high redshift ($z > 5$). Our third, main conclusion is that a heavy seeding mechanism for black holes provides a physically motivated way to increase the predicted number density of very luminous QSOs at high redshift, in line with observations. This is in agreement with the studies of Volonteri et al. (2008) and Volonteri (2010), which showed that either massive black hole seeds are required or less massive seeds have to accrete at super-Eddington rates. Unfortunately, current observational constraints are not sufficient to favor one of these possibilities. This may be possible with the next generation of planned X-ray missions (e.g. WFXT, IXO). As an implicit consequence of massive black hole seeds, we have also assumed that seeds are not able to form in dark matter halos below $2 \times 10^{11}\ M_\odot$, as cold gas might not be able to collapse in these halos due to their shallow potential wells (Volonteri et al. 2008). This simultaneously reduces the number of faint AGN at high redshift, in better agreement with observations.

We find that the FID model with a combination of the above modifications (=VEDISH model) can reproduce the downsizing trend fairly well and is e.g. able to match the observational compilation of Hopkins et al. (2007). Moreover, we have shown that the additional modifications do not change basic galaxy and black hole properties at $z = 0$ significantly and thus, our model galaxies are still in agreement with the observed local stellar mass function, black hole mass function and the black hole-bulge mass relation. However, as in other semi-analytic models we find that at high redshift ($z \gtrsim 1$) the number of low-mass galaxies at high redshift is overestimated and the number of high-mass galaxies may be underestimated. These predictions are insensitive to our modifications to the black hole seeding and growth recipes, but of course our predictions for AGN number densities are impacted by these discrepancies in correctly predicting the galaxy population.

For the "best-fit" VEDISH model we find that the peaks of the distributions of Eddington ratios move towards smaller values with decreasing redshift in qualitative agreement with observational studies (Vestergaard 2003; Kollmeier et al. 2006; Netzer & Trakhtenbrot 2007; Kelly et al. 2010; Schulze & Wisotzki 2010). Additionally, the results of the VEDISH model are in excellent agreement with the observed accretion limit in the $L_{\rm bol} - M_\bullet$-plane of Steinhardt & Elvis (2010). In our model, this behavior results from the gas-fraction dependent accretion rate cap that we applied.

Despite the success of the final VEDISH model in reproducing the bolometric AGN luminosity function from the Hopkins compilation, the number of faint AGN still appears to be overestimated at high redshifts $4 > z > 2$. One possible explanation for this discrepancy is a redshift-dependent dust obscuration, which was neglected in Hopkins et al. (2007). Therefore, we have compared our model results directly to the observed AGN LF in the soft- and hard X-ray band by assuming the obscuration model from Hasinger (2008) for the soft- and also for the hard X-ray luminosities, as even $2 - 10$ keV X-ray surveys will miss a significant fraction of moderately obscured AGN and nearly all Compton-thick AGN (Treister et al. 2004; Ballantyne et al. 2006). With our

VEDISH model including obscuration effects we achieve excellent agreement with the observed AGN LF in the soft and hard X-ray bands for the whole luminosity range at *all* redshifts. Therefore, our results suggest that the obscured and Compton-thick AGN missed in deep X-ray surveys likely constitute a significant fraction of the total AGN population at all luminosities, in particular of moderately luminous AGN at high redshift. However, we note that although obscuration effects contribute to the late peak in the number densities of moderately luminous AGN, in our model they *cannot* account for the observed downsizing trend completely (see FID model and dust obscuration in Figs. 9 and 8).

Comparing our conclusions with those of some previous studies (see Section 2), we summarize the following main points: Marulli et al. (2008) found that a model based on the original MUNICH semi-analytic code and BH growth recipe (Kauffmann & Haehnelt 2000; Croton 2006), and with a light curve model similar to the one adopted here, underproduced luminous AGN at high redshift and slightly overproduced them at low redshift ($z \sim 0$), and underproduced low-luminosity AGN at low redshift ($z \lesssim 1$). As a result, they introduced an ad-hoc scaling of the black hole accretion efficiency with an explicit redshift dependence. With this "best fit" model, they were able to reproduce the bolometric AGN luminosity function fairly well except at very high redshift ($z > 4$). Thus, their results are qualitatively very consistent with ours — in effect, they found that the same qualitative modifications to the model were necessary, and achieved this via an explicit modification of the accretion efficiency, while we have tried to achieve this by adding more physically motivated effects. However, contrary to our study, they find that they do not need AGN activity triggered by disk instabilities, but can explain all AGN activity with a merger model.

In contrast, in the study based on the Durham GALFORM model (Fanidakis et al. 2010), disk instabilities are the major triggering mechanism for black hole activity for *all* luminosities at *all* redshifts. With their model they can reproduce the AGN luminosity function at all redshifts: the low-luminosity end of the AGN luminosity function is mainly due to their ADAF model (cold gas accretion onto the black hole in a hot halo), whereas in our model it is due to accretion in the power-law decline regime as well as black hole accretion from disk instabilities. At high redshift, they predict that super-Eddington accretion is responsible for producing luminous AGN. At this point, it is not clear whether a heavy seeding mechanism (as assumed in this study) or super-Eddington accretion describes the correct physical processes. For that question, the improvement of high-redshift AGN observations will be of crucial importance, both by enlarging the current high-z AGN samples and by reducing the current uncertainty originating from incompleteness problems. They mainly attribute the downsizing trend to dust obscuration effects.

Thus the main triggering mechanism of most of the black hole growth in the universe remains a major open question. It is clear that with the allowed freedoms from various modeling and observational uncertainties, it is possible to reproduce the *number densities* of AGN (luminosity functions) as a function of redshift within a range of scenarios, from a pure merger scenario, to a hybrid merger+disk instability scenario such as the one we have suggested, to a pure disk-instability driven scenario. Hopefully, this issue will be clarified by further studies of the morphology of AGN hosts, now possible out to the peak of luminous AGN activity $z \sim 2$ with Wide Field Camera 3 (WFC3) on Hubble (e.g. Schawinski et al. 2011; Kocevski et al. 2012; Rosario et al. 2011), and the enhancement of AGN activity in close pairs over a range of redshifts and luminosities. We intend to make a more quantitative comparison of our predicted host properties with observations in a future work.

Overall, we conclude that the models presented here provide a plausible attempt to understand the complex scenario of black hole and galaxy co-evolution, and to predict the downsizing trend within the framework of hierarchical clustering. However, there still remain many uncertainties in modelling the formation and evolution of black holes, which hopefully ongoing and future observational facilities will help to constrain.

ACKNOWLEDGMENTS

This research was supported by the DFG Cluster of Excellence 'Origin and structure of the universe'. MH acknowledges financial support from the European Research Council under the European Community's Seventh Framework Programme (FP7/2007-2013)/ERC grant agreement n. 202781. We thank Francesco Shankar, James Aird, Jacobo Ebrero and Fabrizio Fiore for providing us with observational data and David Alexander, Fabrizio Fiore, Francesco Shankar, Phil Hopkins, Brant Robertson, TJ Cox, Lars Hernquist, and Yuexing Li for fruitful discussions.

REFERENCES

Aird J., Nandra K., Laird E. S., Georgakakis A., Ashby M. L. N., Barmby P., Coil A. L., Huang J., Koekemoer A. M., Steidel C. C., Willmer C. N. A., 2010, MNRAS, 401, 2531

Ballantyne D. R., Shi Y., Rieke G. H., Donley J. L., Papovich C., Rigby J. R., 2006, ApJ, 653, 1070

Barger A. J., Cowie L. L., 2005, ApJ, 635, 115

Barger A. J., Cowie L. L., Capak P., Alexander D. M., Bauer F. E., Brandt W. N., Garmire G. P., Hornschemeier A. E., 2003, ApJ, 584, L61

Bell E. F., McIntosh D. H., Katz N., Weinberg M. D., 2003, ApJ, 585, L117

Bellovary J., Volonteri M., Governato F., Shen S., Quinn T., Wadsley J., 2011, ApJ, 742, 13

Blumenthal G. R., Faber S. M., Primack J. R., Rees M. J., 1985, Nature, 313, 72

Bondi H., 1952, MNRAS, 112, 195

Bonoli S., Marulli F., Springel V., White S. D. M., Branchini E., Moscardini L., 2009, MNRAS, 396, 423

Bournaud F., Dekel A., Teyssier R., Cacciato M., Daddi E., Juneau S., Shankar F., 2011, ApJ, 741, L33

Bower R. G., Benson A. J., Crain R. A., 2011, ArXiv e-prints

Bower R. G., Benson A. J., Malbon R., Helly J. C., Frenk C. S., Baugh C. M., Cole S., Lacey C. G., 2006, MNRAS, 370, 645

Boyle B. J., Shanks T., Croom S. M., Smith R. J., Miller L., Loaring N., Heymans C., 2000, MNRAS, 317, 1014
Boyle B. J., Shanks T., Peterson B. A., 1988, MNRAS, 235, 935
Bromley J. M., Somerville R. S., Fabian A. C., 2004, MNRAS, 350, 456
Bundy K., Ellis R. S., Conselice C. J., 2005, ApJ, 625, 621
Ceverino D., Dekel A., Bournaud F., 2010, MNRAS, 404, 2151
Cisternas M., Jahnke K., Inskip K. J., Inskip 2010, in IAU Symposium Vol. 267 of IAU Symposium, Quasars Do Not Live in Merging Systems: No Enhanced Merger Rate at z $<$ 0.8. pp 326–326
Cowie L. L., Barger A. J., Bautz M. W., Brandt W. N., Garmire G. P., 2003, ApJ, 584, L57
Cox T. J., Dutta S. N., Di Matteo T., Hernquist L., Hopkins P. F., Robertson B., Springel V., 2006a, ApJ, 650, 791
Cox T. J., Dutta S. N., Di Matteo T., Hernquist L., Hopkins P. F., Robertson B., Springel V., 2006b, ApJ, 650, 791
Cristiani S., Alexander D. M., Bauer F., Brandt W. N., Chatzichristou E. T., Fontanot F., Grazian A., Koekemoer A., Lucas R. A., Monaco P., Nonino M., Padovani P., Stern D., Tozzi P., Treister E., Urry C. M., Vanzella E., 2004, ApJ, 600, L119
Croom S. M., Smith R. J., Boyle B. J., Shanks T., Miller L., Outram P. J., Loaring N. S., 2004, MNRAS, 349, 1397
Croton D. J., 2006, MNRAS, 369, 1808
Davé R., Oppenheimer B. D., Finlator K., 2011, ArXiv:1103.3528
De Lucia G., Blaizot J., 2007, MNRAS, 375, 2
Degraf C., Di Matteo T., Springel V., 2011, MNRAS, 413, 1383
Di Matteo T., Khandai N., DeGraf C., Feng Y., Croft R. A. C., Lopez J., Springel V., 2012, ApJ, 745, L29
Di Matteo T., Springel V., Hernquist L., 2005, Nature, 433, 604
Drory N., Bender R., Feulner G., Hopp U., Maraston C., Snigula J., Hill G. J., 2004, ApJ, 608, 742
Ebrero J., Carrera F. J., Page M. J., Silverman J. D., Barcons X., Ceballos M. T., Corral A., Della Ceca R., Watson M. G., 2009, A&A, 493, 55
Efstathiou G., Lake G., Negroponte J., 1982, MNRAS, 199, 1069
Efstathiou G., Rees M. J., 1988, MNRAS, 230, 5P
Ellison S. L., Patton D. R., Mendel J. T., Scudder J. M., 2011, MNRAS, 418, 2043
Ellison S. L., Patton D. R., Simard L., McConnachie A. W., 2008, AJ, 135, 1877
Fan X., Hennawi J. F., Richards G. T., Strauss M. A., Schneider D. P., Donley J. L., Young J. E., Annis J., Lin H., Lampeitl H., Lupton R. H., Gunn J. E., Knapp G. R., 2004, AJ, 128, 515
Fan X., Narayanan V. K., Lupton R. H., Strauss M. A., Knapp G. R., Becker R. H., White R. L., Pentericci L., Leggett S. K., Haiman Z., Gunn J. E., Ivezić Ž., Schneider D. P., Anderson S. F., 2001, AJ, 122, 2833
Fan X., White R. L., Davis M., Becker R. H., Strauss M. A., Haiman Z., Schneider D. P., Gregg M. D., Gunn J. E., Knapp G. R., Lupton R. H., Anderson Jr. J. E., Anderson S. F., Annis J., Bahcall N. A., Boroski W. N., 2000, AJ, 120, 1167
Fanidakis N., Baugh C. M., Benson A. J., Bower R. G., Cole S., Done C., Frenk C. S., Hickox R. C., Lacey C., Lagos C. d. P., 2010, ArXiv:1011.5222
Ferrarese L., Merritt D., 2000, ApJ, 539, L9
Fiore F., Brusa M., Cocchia F., Baldi A., Carangelo N., Ciliegi P., Comastri A., La Franca F., Maiolino R., Matt G., Molendi S., Mignoli M., Perola G. C., Severgnini P., Vignali C., 2003, A&A, 409, 79
Fiore F., Puccetti S., Grazian A., Menci N., Shankar F., Santini P., Piconcelli E., Koekemoer A. M., Fontana A., Boutsia K., Castellano M., Lamastra A., Malacaria C., Feruglio C., Mathur S., Miller N., Pannella M., 2012, A&A, 537, A16
Fontana A., Salimbeni S., Grazian A., Giallongo E., Pentericci L., Nonino M., Fontanot F., Menci N., Monaco P., Cristiani S., Vanzella E., de Santis C., Gallozzi S., 2006, A&A, 459, 745
Fontanot F., De Lucia G., Monaco P., Somerville R. S., Santini P., 2009, MNRAS, 397, 1776
Fontanot F., Monaco P., Cristiani S., Tozzi P., 2006, MNRAS, 373, 1173
Fontanot F., Pasquali A., De Lucia G., van den Bosch F. C., Somerville R. S., Kang X., 2011, MNRAS, pp 198–+
Gebhardt K., Bender R., Bower G., Dressler A., Faber S. M., Filippenko A. V., Green R., Grillmair C., Ho L. C., Kormendy J., Lauer T. R., Magorrian J., Pinkney J., Richstone D., Tremaine S., 2000, ApJ, 539, L13
Genzel R., Eckart A., 1999, in H. Falcke, A. Cotera, W. J. Duschl, F. Melia, & M. J. Rieke ed., The Central Parsecs of the Galaxy Vol. 186 of Astronomical Society of the Pacific Conference Series, The Galactic Center Black Hole. pp 3–+
Georgakakis A., Coil A. L., Laird E. S., Griffith R. L., Nandra K., Lotz J. M., Pierce C. M., Cooper M. C., Newman J. A., Koekemoer A. M., 2009, MNRAS, 397, 623
Gilli R., Comastri A., Hasinger G., 2007, A&A, 463, 79
Gilli R., Tozzi P., Rosati P., Paolillo M., Borgani S., Brusa M., Comastri A., Lusso E., Marulli F., Vignali C., 2010, ArXiv:1010.6024
Granato G. L., De Zotti G., Silva L., Bressan A., Danese L., 2004, ApJ, 600, 580
Greene J. E., Peng C. Y., Ludwig R. R., 2010, ApJ, 709, 937
Grogin N. A., Conselice C. J., Chatzichristou E., Alexander D. M., Bauer F. E., Hornschemeier A. E., Jogee S., Koekemoer A. M., Laidler V. G., Livio M., Lucas R. A., Paolillo M., Ravindranath S., Schreier E. J., Simmons B. D., Urry C. M., 2005, ApJ, 627, L97
Guo Q., White S., Boylan-Kolchin M., De Lucia G., Kauffmann G., Lemson G., Li C., Springel V., Weinmann S., 2011, MNRAS, pp 164–+
Haehnelt M. G., Rees M. J., 1993, MNRAS, 263, 168
Haiman Z., 2010, in D. J. Whalen, V. Bromm, & N. Yoshida ed., American Institute of Physics Conference Series Vol. 1294 of American Institute of Physics Conference Series, The Origin and Detection of High-Redshift Supermassive Black Holes. pp 215–224
Haiman Z., Loeb A., 1998, ApJ, 503, 505
Häring N., Rix H.-W., 2004, ApJ, 604, L89
Hasinger G., 2004, Nuclear Physics B Proceedings Supplements, 132, 86

Hasinger G., 2008, A&A, 490, 905
Hasinger G., Miyaji T., Schmidt M., 2005, A&A, 441, 417
Heger A., Woosley S. E., 2002, ApJ, 567, 532
Hewett P. C., Irwin M. J., Foltz C. B., Harding M. E., Corrigan R. T., Webster R. L., Dinshaw N., 1994, AJ, 108, 1534
Hickox R. C., Jones C., Forman W. R., Murray S. S., Kochanek C. S., Eisenstein D., Jannuzi B. T., Dey A., Brown M. J. I., Stern D., Eisenhardt P. R., Gorjian V., Brodwin M., Narayan R., Cool R. J., Kenter A., Caldwell N., Anderson M. E., 2009, ApJ, 696, 891
Hirschmann M., Khochfar S., Burkert A., Naab T., Genel S., Somerville R. S., 2010, MNRAS, 407, 1016
Hirschmann M., Naab T., Somerville R., Burkert A., Oser L., 2011, ArXiv:1104.1626
Hopkins P. F., Cox T. J., Kereš D., Hernquist L., 2008, ApJS, 175, 390
Hopkins P. F., Hernquist L., 2009, ApJ, 694, 599
Hopkins P. F., Hernquist L., Cox T. J., Kereš D., 2008, ApJS, 175, 356
Hopkins P. F., Hernquist L., Cox T. J., Robertson B., Di Matteo T., Springel V., 2006, ApJ, 639, 700
Hopkins P. F., Hernquist L., Cox T. J., Robertson B., Krause E., 2007a, ApJ, 669, 45
Hopkins P. F., Hernquist L., Cox T. J., Robertson B., Krause E., 2007b, ApJ, 669, 67
Hopkins P. F., Richards G. T., Hernquist L., 2007, ApJ, 654, 731
Hopkins P. F., Robertson B., Krause E., Hernquist L., Cox T. J., 2006, ApJ, 652, 107
Hunt M. P., Steidel C. C., Adelberger K. L., Shapley A. E., 2004, ApJ, 605, 625
Ilbert O., Salvato M., Le Floc'h E., Aussel H., Capak P., McCracken H. J., Mobasher B., Kartaltepe J., Scoville N., Sanders D. B., 2010, ApJ, 709, 644
Jogee S., Miller S., Penner K., Bell E. F., Conselice C., Skelton R. E., Somerville R. S., Rix H., Barazza F. D., 2008, in J. G. Funes & E. M. Corsini ed., Formation and Evolution of Galaxy Disks Vol. 396 of Astronomical Society of the Pacific Conference Series, Frequency and Impact of Galaxy Mergers and Interactions over the Last 7 Gyr. pp 337–+
Johansson P. H., Naab T., Burkert A., 2009, ApJ, 690, 802
Kauffmann G., Haehnelt M., 2000, MNRAS, 311, 576
Kelly B. C., Vestergaard M., Fan X., Hopkins P., Hernquist L., Siemiginowska A., 2010, ApJ, 719, 1315
Kimm T., Somerville R. S., Yi S. K., van den Bosch F. C., Salim S., Fontanot F., Monaco P., Mo H., Pasquali A., Rich R. M., Yang X., 2009, MNRAS, 394, 1131
King A., 2005, ApJ, 635, L121
Kocevski D. D., Faber S. M., Mozena M., Koekemoer A. M., Nandra K., Rangel C., Laird E. S., Brusa M., Wuyts S., Trump J. R., Koo D. C., Somerville R. S., Bell E. F., Lotz J. M., Alexander D. M., Bournaud F., Conselice C. J., Dahlen T., 2012, ApJ, 744, 148
Kollmeier J. A., Onken C. A., Kochanek C. S., Gould A., Weinberg D. H., Dietrich M., Cool R., Dey A., Eisenstein D. J., Jannuzi B. T., Le Floc'h E., Stern D., 2006, ApJ, 648, 128
Koushiappas S. M., Bullock J. S., Dekel A., 2004, MNRAS, 354, 292
Koushiappas S. M., Zentner A. R., 2006, ApJ, 639, 7
La Franca F., Fiore F., Comastri A., Perola G. C., Sacchi N., Brusa M., Cocchia F., Feruglio C., Matt G., Vignali C., Carangelo N., Ciliegi P., Lamastra A., Maiolino R., Mignoli M., Molendi S., Puccetti S., 2005, ApJ, 635, 864
La Franca F., Matute I., Fiore F., Gruppioni C., Pozzi F., Vignali C., The Hellas Elais Consortii 2002, in R. Maiolino, A. Marconi, & N. Nagar ed., Issues in Unification of Active Galactic Nuclei Vol. 258 of Astronomical Society of the Pacific Conference Series, The Evolution of AGNs in the Hard X-Rays and the Infrared. pp 241–+
Li C., Kauffmann G., Heckman T. M., White S. D. M., Jing Y. P., 2008, MNRAS, 385, 1915
Li Y., Hernquist L., Robertson B., Cox T. J., Hopkins P. F., Springel V., Gao L., Di Matteo T., Zentner A. R., Jenkins A., Yoshida N., 2007, ApJ, 665, 187
Loeb A., Rasio F. A., 1994, ApJ, 432, 52
Lotz J. M., Jonsson P., Cox T. J., Croton D., Primack J. R., Somerville R. S., Stewart K., 2011, ApJ, 742, 103
Lu Y., Kereš D., Katz N., Mo H. J., Fardal M., Weinberg M. D., 2011, MNRAS, 416, 660
Lynden-Bell D., 1969, Nature, 223, 690
Madau P., Rees M. J., 2001, ApJ, 551, L27
Magorrian J., Tremaine S., Richstone D., Bender R., Bower G., Dressler A., Faber S. M., Gebhardt K., Green R., Grillmair C., Kormendy J., Lauer T., 1998, AJ, 115, 2285
Maiolino R., Marconi A., Oliva E., 2001, A&A, 365, 37
Maiolino R., Oliva E., Ghinassi F., Pedani M., Mannucci F., Mujica R., Juarez Y., 2004, A&A, 420, 889
Malbon R. K., Baugh C. M., Frenk C. S., Lacey C. G., 2007, MNRAS, 382, 1394
Marchesini D., van Dokkum P., Quadri R., Rudnick G., Franx M., Lira P., Wuyts S., Gawiser E., Christlein D., Toft S., 2007, ApJ, 656, 42
Marchesini D., van Dokkum P. G., 2007, ApJ, 663, L89
Marconi A., Risaliti G., Gilli R., Hunt L. K., Maiolino R., Salvati M., 2004, MNRAS, 351, 169
Marulli F., Bonoli S., Branchini E., Moscardini L., Springel V., 2008, MNRAS, 385, 1846
Matute I., La Franca F., Pozzi F., Gruppioni C., Lari C., Zamorani G., 2006, A&A, 451, 443
Mayer L., Kazantzidis S., Escala A., Callegari S., 2010, Nature, 466, 1082
McCarthy I. G., Schaye J., Bower R. G., Ponman T. J., Booth C. M., Dalla Vecchia C., Springel V., 2011, MNRAS, 412, 1965
McCarthy I. G., Schaye J., Ponman T. J., Bower R. G., Booth C. M., Dalla Vecchia C., Crain R. A., Springel V., Theuns T., Wiersma R. P. C., 2010, MNRAS, 406, 822
McLure R. J., Jarvis M. J., Targett T. A., Dunlop J. S., Best P. N., 2006, New Astronomy Review, 50, 782
Menci N., Fiore F., Lamastra A., 2012, ArXiv e-prints
Menci N., Fiore F., Perola G. C., Cavaliere A., 2004, ApJ, 606, 58
Menci N., Fiore F., Puccetti S., Cavaliere A., 2008, ApJ, 686, 219
Miyaji T., Hasinger G., Schmidt M., 2000, A&A, 353, 25
Monaco P., Fontanot F., 2005, MNRAS, 359, 283
Mortlock D. J., Warren S. J., Venemans B. P., Patel M., Hewett P. C., McMahon R. G., Simpson C., Theuns T., Gonzáles-Solares E. A., Adamson A., Dye S., Hambly N. C., Hirst P., Irwin M. J., Kuiper E., Lawrence A., Röttgering H. J. A., 2011, Nature, 474, 616

Mullaney J. R., Pannella M., Daddi E., Alexander D. M., Elbaz D., Hickox R. C., Bournaud F., Altieri B., Aussel H., Coia D., Dannerbauer H., Dasyra K., 2012, MNRAS, 419, 95
Murray N., Quataert E., Thompson T. A., 2005, ApJ, 618, 569
Nandra K., Laird E. S., Steidel C. C., 2005, MNRAS, 360, L39
Netzer H., Trakhtenbrot B., 2007, ApJ, 654, 754
Nulsen P. E. J., Fabian A. C., 2000, MNRAS, 311, 346
Padovani P., 1989, A&A, 209, 27
Panter B., Jimenez R., Heavens A. F., Charlot S., 2007, MNRAS, 378, 1550
Peebles P. J. E., 1965, ApJ, 142, 1317
Peng C. Y., Impey C. D., Ho L. C., Barton E. J., Rix H.-W., 2006, ApJ, 640, 114
Pérez-González P. G., Rieke G. H., Villar V., Barro G., Blaylock M., Egami E., Gallego J., Gil de Paz A., Pascual S., Zamorano J., Donley J. L., 2008, ApJ, 675, 234
Pierce C. M., Lotz J. M., Laird E. S., Lin L., Nandra K., Primack J. R., Faber S. M., Barmby P., Park S. Q., Willner S. P., Gwyn S., Koo D. C., Coil A. L., Cooper M. C., Georgakakis A., Koekemoer A. M., Noeske K. G., Weiner B. J., Willmer C. N. A., 2007, ApJ, 660, L19
Richards G. T., Strauss M. A., Fan X., Hall P. B., Jester S., Schneider D. P., Vanden Berk D. E., Stoughton C., Anderson S. F., Brunner R. J., Gray J., Gunn J. E., 2006, AJ, 131, 2766
Robertson B., Bullock J. S., Cox T. J., Di Matteo T., Hernquist L., Springel V., Yoshida N., 2006, ApJ, 645, 986
Robertson B., Cox T. J., Hernquist L., Franx M., Hopkins P. F., Martini P., Springel V., 2006, ApJ, 641, 21
Robertson B., Hernquist L., Cox T. J., Di Matteo T., Hopkins P. F., Martini P., Springel V., 2006, ApJ, 641, 90
Rosario D. J., Mozena M., Wuyts S., Nandra K., Koekemoer A., McGrath E., Hathi N., Dekel A., Donley J., Dunlop J. S., Faber S. M., Ferguson H., Giavalisco M., Grogin N., Guo Y., Newman J., Kocevski D. D., Koo D. C., Somerville R., 2011, ArXiv e-prints
Salpeter E. E., 1964, ApJ, 140, 796
Sazonov S. Y., Revnivtsev M. G., 2004, A&A, 423, 469
Schawinski K., Treister E., Urry C. M., Cardamone C. N., Simmons B., Yi S. K., 2011, ApJ, 727, L31
Schmidt M., Green R. F., 1983, ApJ, 269, 352
Schmidt M., Schneider D. P., Gunn J. E., 1995, AJ, 110, 68
Schramm M., Wisotzki L., Jahnke K., 2008, A&A, 478, 311
Schulze A., Wisotzki L., 2010, A&A, 516, A87+
Sesana A., Haardt F., Madau P., Volonteri M., 2005, ApJ, 623, 23
Shankar F., 2009, NewAR, 53, 57
Shankar F., Marulli F., Mathur S., Bernardi M., Bournaud F., 2012, A&A, 540, A23
Shankar F., Salucci P., Granato G. L., De Zotti G., Danese L., 2004, MNRAS, 354, 1020
Shankar F., Weinberg D. H., Miralda-Escudé J., 2009, ApJ, 690, 20
Shankar F., Weinberg D. H., Miralda-Escude' J., 2011, ArXiv e-prints
Shankar F., Weinberg D. H., Shen Y., 2010, ArXiv:1004.1173
Sijacki D., Springel V., Di Matteo T., Hernquist L., 2007, MNRAS, 380, 877
Silverman J. D., Kampczyk P., Jahnke K., Andrae R., Lilly S. J., Elvis M., Civano F., Mainieri V., Vignali C., Zamorani G., Nair P., Le Fèvre O., de Ravel L., Bardelli S., Bongiorno A., 2011, ApJ, 743, 2
Sivakoff G. R., Gilli R., Brandt W. N., Hickox R. C., Murray S. S., Ptak A., Wide Field X-Ray Telescope Team 2010, in Bulletin of the American Astronomical Society Vol. 42 of Bulletin of the American Astronomical Society, Understanding The Growth And Evolution Of Super Massive Black Holes With The Wide Field X-ray Telescope. pp 520–+
Soltan A., 1982, MNRAS, 200, 115
Somerville R. S., Gilmore R. C., Primack J. R., Dominguez A., 2011, ArXiv e-prints
Somerville R. S., Hopkins P. F., Cox T. J., Robertson B. E., Hernquist L., 2008, MNRAS, 391, 481
Springel V., Di Matteo T., Hernquist L., 2005, MNRAS, 361, 776
Steffen A. T., Barger A. J., Cowie L. L., Mushotzky R. F., Yang Y., 2003, ApJ, 596, L23
Steinhardt C. L., Elvis M., 2010, MNRAS, 402, 2637
Tanaka T., Haiman Z., 2009, ApJ, 696, 1798
Treister E., Urry C. M., Chatzichristou E., Bauer F., Alexander D. M., Koekemoer A., Van Duyne J., Brandt W. N., Bergeron J., Stern D., Moustakas L. A., Chary R., Conselice C., Cristiani S., Grogin N., 2004, ApJ, 616, 123
Tremaine S., Gebhardt K., Bender R., Bower G., Dressler A., Faber S. M., Filippenko A. V., Green R., Grillmair C., Ho L. C., Kormendy J., Lauer T. R., Magorrian J., Pinkney J., Richstone D., 2002, ApJ, 574, 740
Ueda Y., Akiyama M., Ohta K., Miyaji T., 2003, ApJ, 598, 886
Vestergaard M., 2003, ApJ, 599, 116
Volonteri M., 2010, A&A Rev., 18, 279
Volonteri M., Dotti M., Campbell D., Mateo M., 2011, ApJ, 730, 145
Volonteri M., Haardt F., Madau P., 2003, ApJ, 582, 559
Volonteri M., Lodato G., Natarajan P., 2008, MNRAS, 383, 1079
Volonteri M., Stark D. P., 2011, MNRAS, 417, 2085
Walter F., Carilli C., Bertoldi F., Menten K., Cox P., Lo K. Y., Fan X., Strauss M. A., 2004, ApJ, 615, L17
Wang L., Weinmann S. M., Neistein E., 2011, ArXiv e-prints
Warren S. J., Hewett P. C., Osmer P. S., 1994, ApJ, 421, 412
White S. D. M., Rees M. J., 1978, MNRAS, 183, 341
Wolf C., Wisotzki L., Borch A., Dye S., Kleinheinrich M., Meisenheimer K., 2003, A&A, 408, 499
Zel'Dovich Y. B., 1964, Soviet Physics Doklady, 9, 195